ISTANBUL TECHNICAL UNIVERSITY ★ ENERGY INSTITUTE

MODELING THE BEHAVIOUR OF CARBON DIOXIDE CONTENT IN GEOTHERMAL RESERVOIRS USING MULTIPLE TANK LUMPED PARAMETER MODELS

M.Sc. THESIS

Alper Süleyman CAN

Energy Science and Technology Division
Energy Science and Technology Programme

DECEMBER 2018

ISTANBUL TECHNICAL UNIVERSITY ★ ENERGY INSTITUTE

MODELING THE BEHAVIOUR OF CARBON DIOXIDE CONTENT IN GEOTHERMAL RESERVOIRS USING MULTIPLE TANK LUMPED PARAMETER MODELS

M.Sc. THESIS

Alper Süleyman CAN
(301161001)

Energy Science and Technology Division
Energy Science and Technology Programme

Thesis Advisor: Assoc. Prof. Dr. Ömer İnanç TÜREYEN

DECEMBER 2018

İSTANBUL TEKNİK ÜNİVERSİTESİ ★ ENERJİ ENSTİTÜSÜ

JEOTERMAL REZERVUARLARDA KARBONDİOKSİT MİKTARININ ÇOKLU TANK MODELİ İLE MODELLENMESİ

YÜKSEK LİSANS TEZİ

Alper Süleyman CAN
(301161001)

Enerji Bilim ve Teknoloji Anabilim Dalı
Enerji Bilim ve Teknoloji Programı

Tez Danışmanı: Doç. Dr. Ömer İnanç TÜREYEN

ARALIK 2018

Alper Süleyman Can, a M.Sc student of ITU Institute of Energy, student ID 301161001, successfully defended the thesis entitled "MODELING THE BEHAVIOUR OF CARBON DIOXIDE CONTENT IN GEOTHERMAL RESERVOIRS USING MULTIPLE TANK LUMPED PARAMETER MODELS", which he prepared after fulfilling the requirements specified in the associated legislation, before the jury whose signatures are below.

Thesis Advisor:	**Assoc. Prof. Dr. Ömer İnanç TÜREYEN** Istanbul Technical University	.....
Jury Members:	**Assoc. Prof. Dr. Didem Korkmaz BAŞEL** Istanbul Technical University	.....
	Prof. Dr. Serhat AKIN Middle East Technical University	.....

Date of Submission : 16 November 2018
Date of Defense : 11 December 2018

To the memory of my beloved grandmother Altın Yüksel,

FOREWORD

First of all, I would like to thank my advisor Assoc. Prof. Dr. Ömer İnanç Türeyen for his generous understanding, help at his lectures, for spending time and guiding me with patience, for motivating me whenever I did not know what to do, and for making me believe that I can understand. I would also like to thank my jury members Assoc. Prof. Dr. Didem Korkmaz Başel and Prof. Dr. Serhat Akın for their advice and suggestions about the thesis. I also want to thank Prof. Dr. Abdurrahman Satman for teaching the fundamentals of reservoir engineering and for his belief in me. I want to thank also to Istanbul Technical University, Institute of Energy. Also, I would like to thank Assoc. Prof. Dr. Coşkun Fırat for making me think from another perspective and for his motivational help in Mathematics. I would also like to thank Petroleum Engineering research assistants Said Ergül and Mehmet Emin Onay for their support, sharing their thoughts and ideas with me. I would also like to thank Umur Alpay who had endless patience and for his full support throughout the thesis, and Meltem Kutnu for making me stay positive throughout the thesis, keeping motivating me and being an inspiration source for me. I would also like to thank my uncle Sirhan Yüksel for his brilliant and genius ideas. And finally, I would like to thank my mother Emine Can and my father Mehmet Korhan Can for their love, understanding, and support.

December 2018

Alper Süleyman Can
(Geology Engineering, B.Sc.)

TABLE OF CONTENTS

Page

ABBREVIATIONS

CO_2	**:** Carbon dioxide
EGS	**:** Enhanced geothermal system
MW	**:** MegaWatt
NCG	**:** Noncondensible gas
ODE	**:** Ordinary differential equation
TW	**:** TeraWatt
W	**:** Watt

Subscripts

0	**:** Initial
b	**:** Bulk
ci	**:** Connected to tank i
E	**:** Residual vector for energy balance
e	**:** Residual vector for energy balance
f	**:** Fluid
inj	**:** Injection
m	**:** Matrix
ni	**:** Connections between tank i other tanks
p	**:** Production
r	**:** Rock
re	**:** Recharge
T	**:** Thermal
t	**:** Total
W	**:** Residual vector for mass balance of water
w	**:** Water
WC	**:** Residual vector for mass balance of Carbon dioxide

SYMBOLS

$\boldsymbol{C}$	**:** Specific heat capacity, J/kg.K
$\boldsymbol{c}$	**:** Compressibility, 1/bar
$\boldsymbol{f}$	**:** Mass fraction of CO_2
$\boldsymbol{h}$	**:** Specific enthalpy J/kg
$\boldsymbol{i}$	**:** Grid Block index
$\mathbf{J}$	**:** Jacobian matrix index
$\boldsymbol{j}$	**:** Grid block index
$\boldsymbol{m}$	**:** Mass, kg
$\boldsymbol{N}$	**:** Number of tanks
$\boldsymbol{p}$	**:** Pressure, bar, Mpa or barg
$\boldsymbol{Q}$	**:** Energy Rate, J/s
$\mathbf{r}$	**:** Residual vector
$\boldsymbol{T}$	**:** Temperature, ^{o}C or K
$\boldsymbol{t}$	**:** Time, seconds
$\boldsymbol{u}$	**:** Specific Internal Energy, J/s
$\boldsymbol{V}$	**:** Volume, m^3
$\boldsymbol{w}$	**:** Mass flow rate, kg/s

Greek Letters

$\boldsymbol{\alpha}$	**:** Recharge index, kg/bar.s
$\boldsymbol{\gamma}$	**:** Conduction index, J/K.s
$\boldsymbol{\Delta}$	**:** Difference operator
$\boldsymbol{\delta}$	**:** Delta vector
$\boldsymbol{\varepsilon}$	**:** Thermal Expansivity, 1/ ^{o}C
$\boldsymbol{\kappa}$	**:** Storage Capacity, kg/bar
$\boldsymbol{\xi}$	**:** Direction
$\boldsymbol{\rho}$	**:** Density, kg/m^3
$\boldsymbol{\phi}$	**:** Porosity

LIST OF TABLES

Page

LIST OF FIGURES

Page

MODELING THE BEHAVIOUR OF CARBON DIOXIDE CONTENT IN GEOTHERMAL RESERVOIRS USING MULTIPLE TANK LUMPED PARAMETER MODELS

SUMMARY

Energy is an essential subject since nothing can be done without energy. For the supply of energy, there is a search for alternative energy sources which are clean, sustainable and renewable. One of the alternative sources is geothermal energy. Geothermal energy is the heat stored underground, that is used for direct uses or electricity generation. The heat is deposited in rock pores and water. Accurate geophysical and geochemical data with observations show whether a field is eligible for geothermal or not. Geothermal energy usage is increasing nowadays for being a clean, sustainable and renewable energy source. Three types of geothermal power plants are considered. Dry steam power plants, flash steam power plants and binary power plants. Turkey is one of the countries in which geothermal energy exits. In, Aydın, Denizli, Manisa regions which are located in the west of Turkey, there are geothermal power plants. Turkey has vast sources, and the amount of energy demand will increase in years with the development of geothermal energy. In order to use geothermal energy efficiently; good reservoir engineering must be practiced.

In a geothermal reservoir, noncondensable gases such as carbon dioxide exist. All geothermal fields in Turkey contain different amounts of carbon dioxide. Carbon dioxide has considerable effect in geothermal reservoirs. Even small portions of carbon dioxide increase the flashing point of the geothermal water. The carbon dioxide content can change based on the production/reinjection operations in a geothermal field. So the change must be modeled well in order to make predictions for future performance.

In this study, a mathematical model is developed for modeling the changes in the carbon dioxide content. The developed mathematical model which gives the change of carbon dioxide as a function of time is a result of a simple mass balance that can be used over any control volume and is only for liquid-dominated geothermal reservoirs. In this study, a geothermal reservoir is modeled using tanks in which mass balance and energy balance equations are used to model pressure, temperature, and carbondioxide content. The physical parameters of the tanks are bulk volume, porosity, the density of the water and compressibility, recharge mass rate, reinjection mass rate and mass production rate. The model is first validated with existing solutions in the literature. Then the model is used for investigating how the carbondioxide content would change in a reservoir under various production/reinjection scenarios. In all the modeling conducted in this study, the reservoir is represented by two tanks. One tank to represent regions close to the recharge source and the other tank to represent the regions further away from the recharge source. The specific schemes that have been considered in this study are; the effects of the recharge carbondioxide content, the location of the production and

reinjection areas. In all cases considered in this study the reinjection water is assumed to contain no carbondioxide. Results show that the change of carbondioxide content in the reservoir is highly dependent on where the production and reinjection operations are performed. Furthermore, the recharge carbondioxide content also has significant effect.

JEOTERMAL REZERVUARLARDA KARBONDİOKSİT MİKTARININ ÇOKLU TANK MODELİ İLE MODELLENMESİ

ÖZET

Enerji konusu son zamanlarda önemli bir konu halini almaya başladı, eksikliği ise güncel hayat akışında bazı aksaklıklara sebebiyet verebilir. Güncel olarak enerjiye olan ihtiyaç gün geçtikçe artmakla beraber, bugüne kadar süregelen fosil yakıt tüketimi ve çevreye verdiği zararlardan dolayı, alternatif enerji arayışına başlanmıştır. Bu alternatif enerji arayışındaki temel amaç yine aynı şekilde kullanılabilinecek, sürdürülebilir, daha temiz, çevreye daha az zarar verebilecek, yenilenebilir gibi temel özelliklerin de içinde olduğu bir enerji arayışına dönmüştür. Bunlar; rüzgar enerjisi, güneş enerjisi, jeotermal enerji gibi enerji kaynaklarıdır. İşte bu noktada bu temel özellikleri barındıran bir enerji türü olan, jeotermal enerjiye olan ihtiyaç artmıştır. Jeotermal enerji; güvenilir, ucuz, kirlilik yaratmayan, sürdürülebilir ve yenilenebilir bir enerji kaynağıdır.

Türkiye jeotermal enerji açısından oldukça zengin bir ülke olmakla beraber , ülkenin batısında İzmir, Aydın, Denizli, Manisa gibi bölgelerde jeotermal enerji santralleri kurulu olmuş olup, bölgeden alınan verim çok yüksektir. Türkiye'nin jeotermal enerji açısından zengin oluşu, jeoloji ve tektonizmayla alakalıdır. Özellikle Türkiye'nin batısında bulunan Menderes grabeni üzerinde olan yerlerde jeotermal enerji oldukça yaygındır. Tektonik olarak uygunluğun sağlandığı Türkiye'de, önümüzdeki yıllarda jeotermal enerji gelişimini arttırarak sağlayacaktır. Jeotermal enerji temel olarak elektrik üretimi ve doğrudan ısıtma gibi amaçlarla da kullanılsa da kültür balıkçılığı, sera ısıtması, ve termal turizm gibi kullanılma alanları da vardır. Yağışlarla beraber yeraltına inen suyun ve çeşitli gazlarında dahil olduğu maddelerin yerin altında depolanmasıyla beraber, tektonik aktivitelerle kırıklı çatlaklı yapıların oluşup bu maddelerin konveksiyon akımlarıyla belli derinliklere kadar yükselmesi ve bu sıcak kaynağın jeotermal santraller aracılığıyla kullanılması jeotermal enerjinin temelini oluşturur.

Jeotermal Enerjinin daha efektif kullanılabilmesi için jeotermal rezervuar mühendisliğine önem verilmelidir. Bu mühendislik kapsamında oluşturulan modellerin gerçeğe yakın olması veya olabildiğince örtüşmesi çok önemlidir. Literatürde önceki rezervuar modellerinde rezervuar sadece su ihtiva etmekteydi, günümüzde ise suyun içerisinde varolan gazlar da mevcuttur, bunlardan bazıları NH_3, H_2S, CO_2'dir. Kütlece miktarları 9% - 10% civarlarına kadar çıkmaktadır. Bu gazlardan en belirgini ve ülkemizde de görülen karbondiosittir. Kızıldere sahası, Germencik sahası gibi sahaların rezervuarlarında genellikle karbondioksit gözlemlenmiştir. Modellemeler yapıldığında karbondioksitin hesaba katılmaması yanlış sonuçlar doğurabilir. Karbondioksit gazının rezervuar termodinamiğine etkisi, ayrışma basıncını arttırmasıdır. Ayrışma basıncının artması karbondioksitin kısmi basıncının artmasıyla artmaktadır. Bu özelliği de üretimdeki basınç düşümünün çok daha az olmasını sağlar, bu sayede çok küçük miktarlardaki karbondioksit bile rezervuar basıncını ve ayrışma basıncını değiştirebilmektedir. Rezervuarla akalı olan

modellemeler yapılırken literatürde sadece su içeren modellemelerle karşılaşılmaktadır, ancak modellemenin doğru olabilmesi adına bu modellemede kullanılan karbondioksit etkisini de dikkate alıp, gerçeğe yakın sonuçlar ortaya konulmuştur. Ülkemizdeki jeotermal sahalarda da karbondioksit bulunduğundan ve modelin gerçeğe yakın olması önemli olduğundan karbondioksitin dikkate alınması önemlidir.
Bu çalışmada kullanım kolaylığı açısından ve yüksek teknolojiye ihtiyaç duyulmadan sonuç vermesi açısından boyutsuz parametre yöntemi kullanılmıştır. Bu yöntem ile rezervuara giren ve çıkan verilerle beraber rezervuar parametrelerinin, rezervuar üzerindeki etkilerini ve karbondioksit miktarını değiştirdiği gözlemlenmektedir. Bu yöntem ileri bir modellemenin olmadığı durumlarda rezervuar hakkında fikir vermek ve rezervuar durumunu anlamak açısından alternatif olarak gösterilebilir. Modelin oluşumunda rezervuar bir tank olarak varsayılmış olup bu varsayıma dahil olarak rezervuardaki fiziksel parametreler modelin içine entegre edilerek gerçekliğe yakınlık sağlanmıştır. Karbondioksit içeren sahaların tek tank modeliyle ve de basit bir kütle korunum denklemiyle, sabit bir reenjeksiyonla zamana bağlı denkleminin kullanılıp rezervuardaki karbondioksit davranışının açıklanması sağlanmıştır. Genelleştirilmiş bu denklemlerle karbondioksitin zamana bağlı olarak nasıl değiştiğine dair bilgi edinilebilmektedir. Bu sistemin gerçeğe yakınlığının sağlanabilmesi için sistem çoklu tanklar için nümerik olarak çözülmüştür. Bu çözüm geliştirilirken, kütle korunum denklemlerinin yanısıra enerji korunum denklemleri de geliştirilmiştir. Ortalama rezervuar basıncı, sıcaklık gibi etmenler de bu denklemlere entegre edilerek karbondioksit miktarı hakkında bilgi edinilmiştir. Su ve karbondioksit için kütle korunum denklemleri ve tüm sistem için enerji korunum denklemleri hesaplanmıştır. Birden fazla diferansiyel denklem nümerik olarak çözülmüştür. Bu denklemler çözülürken Newton – Raphson tekniği kullanılmıştır. Tek tank veya çoklu tank olarak incelenen jeotermal sistemde enerji ve kütle korunum denklemleri her bir tank için beraber çözülmüştür. Sonucunda ise reenjeksiyon, doğal beslenme ve üretim gibi faktörlerin yanısıra sıcaklık ve basınçtaki değişimlere bağlı olan karbondioksit değişimi de incelenmiştir. Denklemler; ayriyetten ısı akışı ve iletimi için modifiye edilerek rezervuardaki performans etkisini gösterecek şekilde ayarlanmıştır. Bu modellemede karbondioksitin zamana bağlı olarak nasıl değiştiği açık bir biçimde gözlemlenmektedir. Model birden fazla tank için kullanılabilir ve farklı değerler için model çalıştırılabilir. Oluşturulan nümerik çözümde, sistem beslenme kaynağına yakın ve beslenme kaynağına uzak olmak üzere iki bölge için incelenmiş ve test edilmiş olup, doğruluğu literatürde bulunan senaryolar ile test edilmiştir.

Bu doğrulamalar hususunda dört önemli sonuç elde edilmiştir:

- Tüm senaryolarda, çok uzun zaman aralıklarında, sistem içerisindeki karbondioksit içeriği kararlı duruma ulaşmaktadır.
- Karbondioksitin kararlı duruma ulaştığı zamandaki sayısal değeri reenjeksiyon içerisindeki karbondioksit içeriği ve beslenme suyundaki karbondioksit içeriğine bağlıdır.
- Reenjeksiyon yapılan karbondioksit içeriği bu çalışmada sıfır olduğundan, re enjeksiyonun yapıldığı bölgelerde de karbondioksit azalımı gözlemlenmektedir.

- Reenjeksiyon içeriğindeki karbondioksit oranı yüksek olduğu zamanlarda, zaman içerisinde daha yüksek karbondioksit oranlarının gözlemlenip elde edilmesine sebep olmuştur.

Tüm çalışılan çoklu sistem senaryolarında, çok uzun zaman aralıklarında sistem kararlı hale gelmiştir, uzun zaman aralıklarında sistemin kararlı hale gelmesinin arkasındaki matematiksel açıklama verilmiştir. Bu çalışmada sistemin kararlı hale gelmesinin matematiksel olarak gösterimine ve karbondioksitin rezervuar içerisindeki zamana bağlı değişimini veren ifadesine yer verilmiştir. Sistem kararlı hale geldiğinde, kararlı haldeki karbondioksitin sayısal değeri, rezervuara reenjeksiyon sırasındaki, reenjeksiyonun içerisindeki karbondioksit miktarına, ve beslenme sırasındaki, beslenme suyu içerisindeki karbondioksit miktarına bağlıdır. Bu şöyle de açıklanabilir: Jeotermal sahalarda su içerisinde bulunan karbondioksit, üretim ile beraber düşmektedir. Bunun genelde iki temel sebebi bulunmaktadır. İlk sebep reenjeksiyon suyunun içerisinde karbondioksit bulunmamasından ötürüdür. Bulunmaması rezervuardaki varolan karbondioksitin seyrelip azalmasına sebebiyet verecektir. İkinci sebep ise; beslenme kaynağı içerisinde karbondioksitin bulunmama durumunda da aynı durum gözlemlenip rezervuardaki varolan karbondioksiti seyreltecektir. Jeotermal sistemde reenjeksiyon işlemi de çok büyük önem arz etmektedir. Sıvı etken jeotermal sahalar için bu yöntemle karbondioksit içeriğinin belirlenmesi sağlanmıştır. Bu çalışmadaki reenjeksiyon içerisindeki karbondioksit değeri sıfır alındığından ötürü reenjeksyonun yapıldığı yerlerde karbondioksit azalımı görülmüştür. Aynı zamanda beslenme içerisindeki karbondioksit miktarı yüksek olduğunda, bunun daha yüksek bir karbondioksit değerine karşılık geldiği sistem içerisinde görünmektedir.

Bu tezde sadece karbondioksit davranışı modellemesi üstünde yoğunlaşılmıştır. Bu çalışmada daha çok farklı sentetik senaryolar içerisindeki farklı üretim ve reenjeksiyon senaryolarına yer verilmiş olup bunların gerçeğe yakın olması açısından nümerik olarak çözümü üzerine yoğunlaşılmıştır. Sekiz adet farklı senaryo incelenmiştir. Bu sentetik senaryoların içerisinde jeotermal rezervuar iki bölümden oluşmaktadır, birinci bölge beslenme kaynağına yakın olan bölge, bir diğeri ise beslenme kaynağına uzak olan bölgedir. Çeşitli senaryolarla bu çalışma gerçekleştirilmiş olup, her senaryoda farklı bir üretim ve reenjeksiyon lokasyonu belirlenip buna göre modelleme sağlanmıştır. Bu dört önemli sonuca göre, bu çalışmada basit bir matematiksel model ile kütle korunum denklemlerinden karbondioksitin zamana bağlı olarak jeotermal bir rezervuarda nasıl değiştiğini gösteren bir denklem üzerinden hareket edilmiştir. Bu denklemden yola çıkılarak, gerçek bir senaryo uygulanması için bu sistem çoklu tank sistemine uygun bir nümerik çözüm ile desteklenmiştir. Nümerik çözüm ile tek bir tank istenilen sayıda tanka veya akifere bağlanabilir veya model istenilen değerler için çalıştırılabilir. Hazırlanan nümerik çözümde üç adet korunum denklemi mevcuttur, bunlar sırasıyla karbondioksit için kütle korunum denklemi, su için kütle korunum denklemi ve toplam enerji korunum denklemi olmak üzere üç adet denklem sistemi oluşturulmuştur. Bu denklemler ile kütle ve enerji korunum denklemlerinin yanısıra jeotermal sistemi farklı bir akifer veya tanka bağlamak için kullanılan bu nümerik çözüm sayesinde tüm denklemler her bir tank için aynı anda çözülmüş olup sistemdeki tüm parametrelerin değişmesi sonucunda sistemdeki toplam karbondioksit, basınç ve sıcaklık gibi parametrelerin nasıl değiştiği hesaplanmıştır. Ancak bu çalışmada sadece karbondioksit miktarı gözlemlenmiştir. Nümerik

çözümün doğruluğu, karbondioksitin zaman bağlı değişimini veren denklemle beraber farklı üretim ve enjeksiyon senaryoları vasıtasıyla test edilmiş ve sonucunda doğruluğu kanıtlanmıştır. Nümerik çözümün uygulanmasının en önemli sebebi karbondioksit miktarını, değişik üretim ve reenjeksiyon hususlarında farklı senaryoların farklı etkileyecek olması durumudur. Bu çalışmada doğal beslenme kaynağına yakın ve doğal beslenme kaynağına uzak olmak üzere iki farklı bölge için çeşitli üretim ve reenjeksiyon senaryolarıyla karbondioksit davranışı modellenmiştir. Bu modelleme sonucunda sıvı etken jeotermal rezervuarlardaki toplam karbondioksit miktarı modellenmiştir. Ulaşılan sonuçlar neticesinde, sentetik olarak farklı şekillerde çoklu tank sistemlerinde yapılan farklı üretim ve reenjeksiyon senaryolarının karbondioksit içeriğini önemli miktarlarda değiştirmiş olduğudur.

1. INTRODUCTION

Nuclear reactions occur in the core of the Earth. As a result of the nuclear reactions, heat is transferred from magma to the upper crust. Aquifers transfer heat to the upper crust or shallow zones by way of convection. Geothermal energy is the heat energy within the earth that is transferred with convection and conduction from deep down to the surface.

Geothermal energy can mainly be used for electricity generation or direct heating (Ghosh and Prelas, 2011). The total amount of 44 TW_T ($44 \times 10^{12} W_T$) of heat power is transferred via convection. 68% of 44 TW_T of power (30 TW_T) is the result from the decay of radioactive elements (Michaelides, 2012). The use of geothermal energy is seen from very early times especially Greeks and Romans who used hot springs and fumaroles as a source of bathing and heating. After this era, geothermal energy evolved, and a resort industry was developed in the 19^{th} century. The electricity production started in 1904 in a small town in Italy called Lardorello. In 1920 the Geysers field had started in North of San Francisco, California and also around 1950s and 1960s 2200 MW_e of total power was being produced. Recently geothermal energy is used for many purposes such as aquaculture, space heating, agriculture and etc. which makes geothermal energy, renewable, sustainable and a reliable source of energy (Michaelides, 2012).

Figure 1.1 shows the internal structure of the Earth. The inner part is the solid iron core and is surrounded by magma. The outer core, which surrounds the inner core, is also surrounded by magma. Continental and oceanic crust are at the lithosphere where tectonic activities occur. The heat flows from the core to the crust. A vast amount of fluid is trapped in pores and fissures of rocks which are heated directly by convection currents (Ghosh and Prelas, 2011).

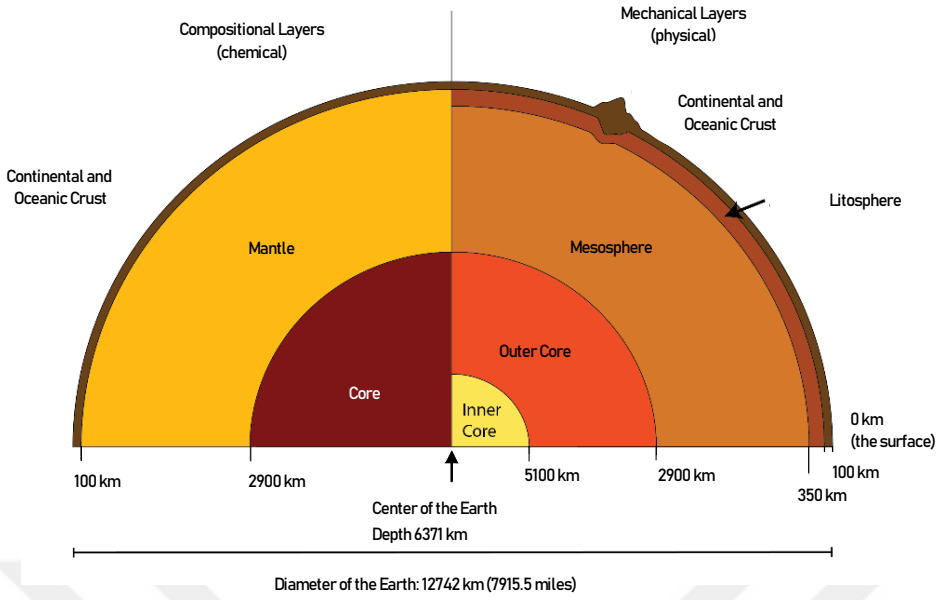

Figure 1.1 : Internal structure of the Earth (Url-1).

Figure 1.2 shows a schematic of the geothermal system. The working mechanism of the geothermal system can be explained with the movement of the convective currents in magma to the upper earth crust; this movement also causes a heat transfer in the system. Tectonic movements in the earth crust cause also forming of faults and fractures through which water can move. When the underground water gets heated, then the convective flow of water takes place in permeable zones. Also permeable rocks act as a trap mechanism and hold the heat within which creates a reservoir. With accurate geophysical and geochemical exploration, geothermal sites are explored.

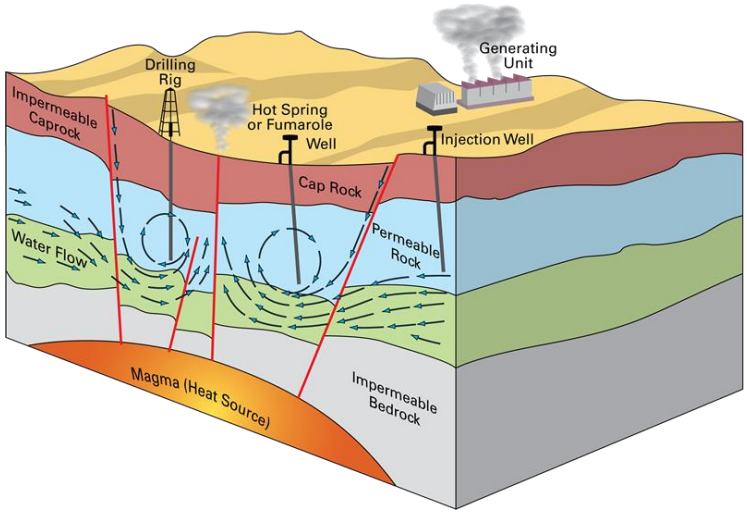

Figure 1.2 : Geothermal system schematic (Url-2).

Tectonically active areas such as subduction zones, spreading ridges, are also indicators of young tectonism and volcanism which can also be found at active plate margins (Muffler, 1993). Also Geysers, fumaroles and hot springs are related indicators of geothermal activities (Acharya, 1983). Figure 1.3 shows the hottest known geothermal regions in the world. As it is seen most of the hot zones are in the Pacific region or as it is called the Ring of Fire region.

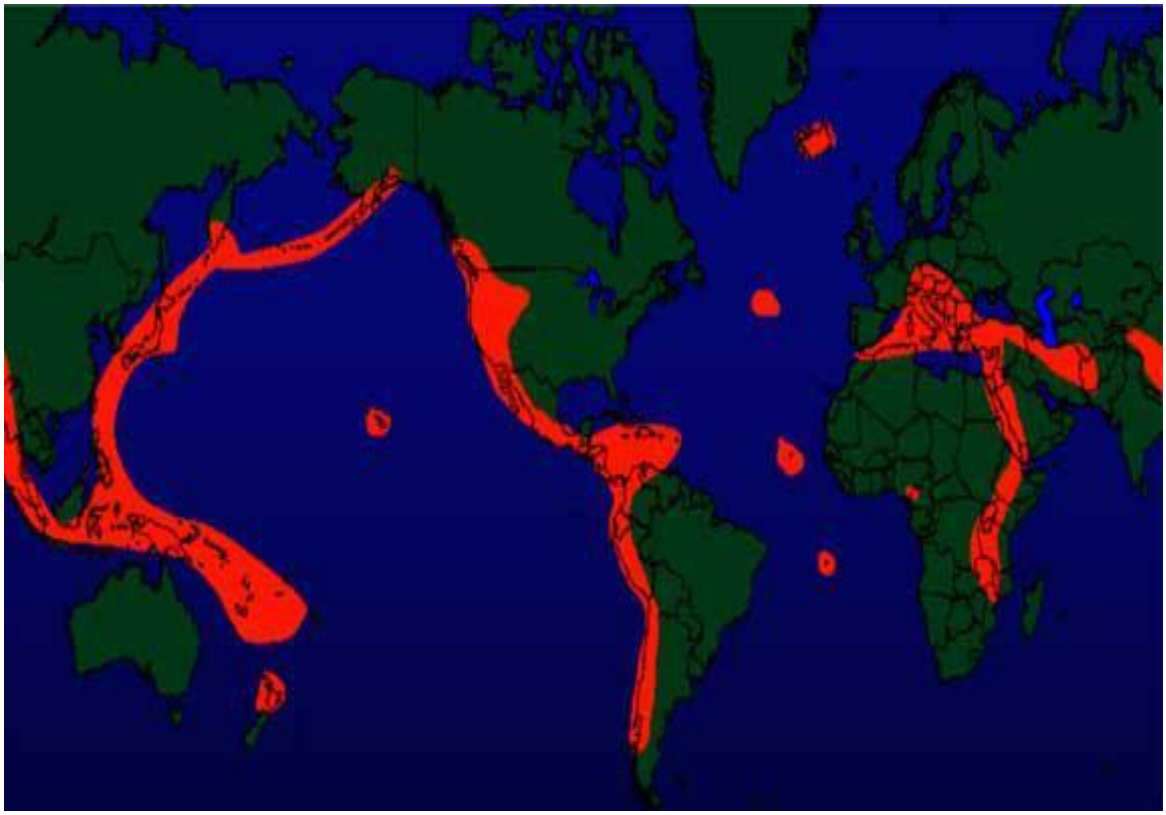

Figure 1.3 : Hottest known geothermal regions (Url-3).

1.1 Geothermal Energy in World

Being a renewable resource geothermal energy usage has started to grow. As being renewable and clean, geothermal energy is used worldwide. In Figure 1.4 it can be seen that the total amount of installed capacity is 14060 MW_e and Top 4 countries which use geothermal energy for power production is: USA, Philippines, Indonesia, and Turkey. With 3591 MW_e United States is number 1 in the list. After the USA, with 1868 MW_e comes the Philippines, The third place is Indonesia which has 1809 MW_e of installed capacity and at the fourth place comes Turkey which has 1100 MW_e of installed capacity (Richter, 2018).

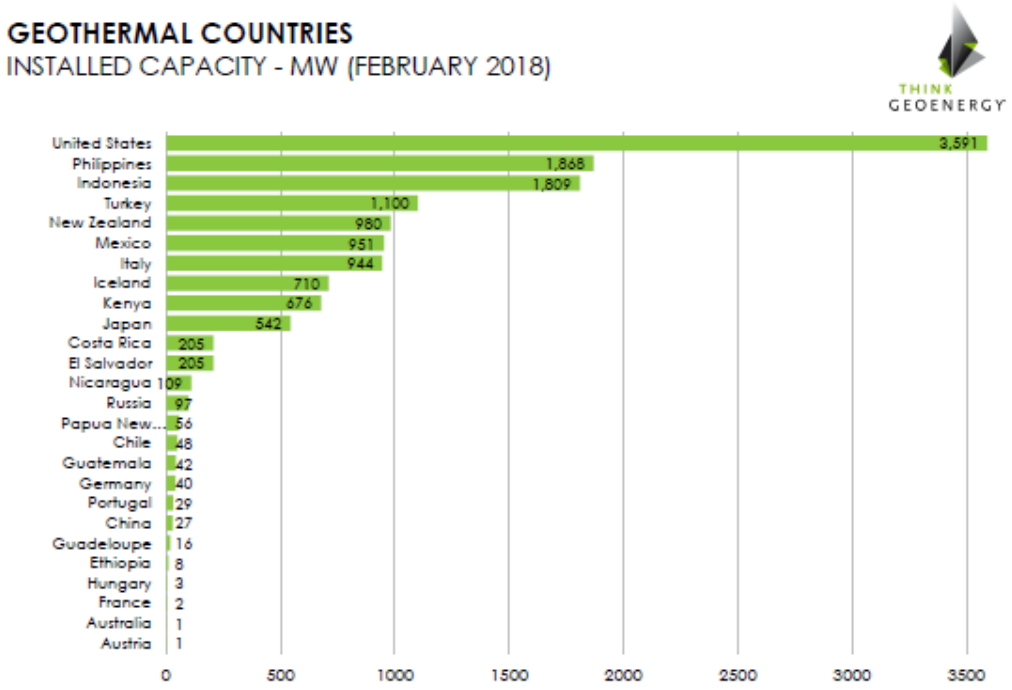

Figure 1.4 : Installed capacity of geothermal energy as of February 2018. Adapted from Richter (2018).

In Figure 1.5, top 10 geothermal countries are given by projects under development. Indonesia has the highest amount among them all with 3958 MW_e , the Philippines is at the second place with 1651 MW_e , at the third place there is USA with 1248 MW_e, Kenya has the fourth place with 1037 MW_e , Ethiopia has the fifth place with 987 MW_e , and Turkey has the sixth place with 798 MW_e **(**Richter, 2018**)**.

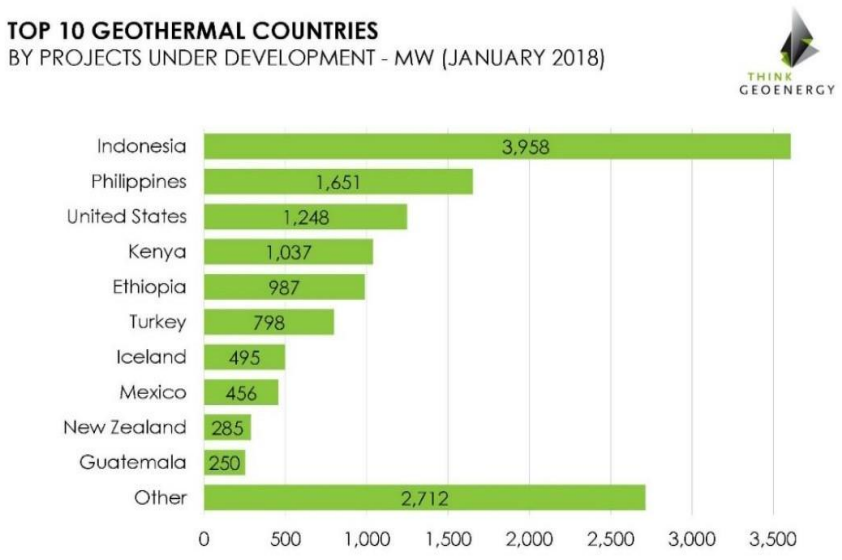

Figure 1.5 : Top 10 geothermal countries as of January 2018. Adapted from Richter (2018).

In Figure 1.6, the global geothermal potential is given. When compared with Figure 1.3, it is seen that the high-temperature regions are the ones which are also tectonically active. In Asia, hydrothermal resources estimates around 70900 MW_e also in North America installed capacity is around 4496 MW_e (Richter, 2018).

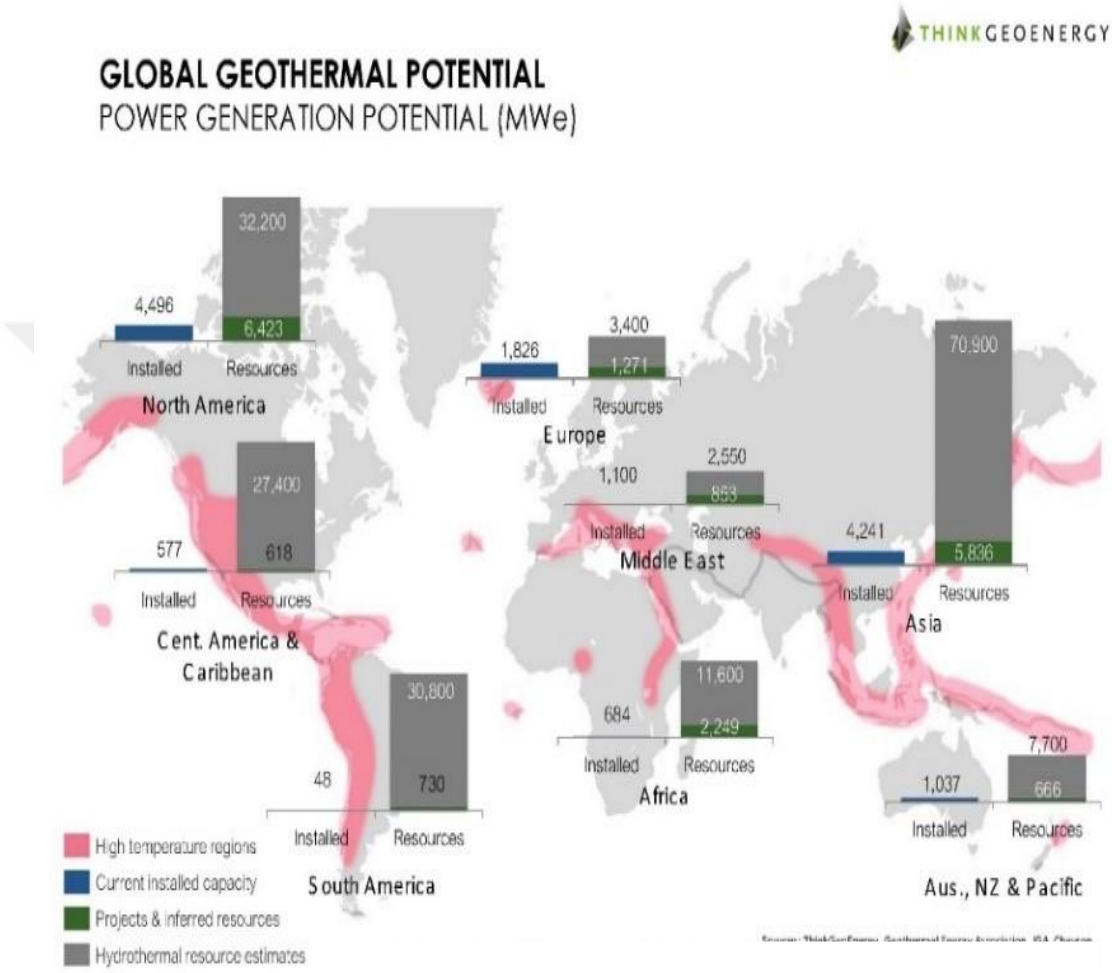

Figure 1.6 : Global geothermal potential. Adapted from Richter (2018).

As can be seen from Figure 1.7 geothermal energy is not just for electric production. Geothermal energy can be in favor of direct use, such as heat pumps, space heating, greenhouse heating, cooling, bathing, and swimming. In direct utilization with heat pumps, the heat pumps occupy 55.3%, space heating occupies 15.01%, bathing and swimming occupies 20.31% whereas without heat pumps bathing and swimming occupy 44.74%, space heating occupies 36.98% in the direct use of geothermal energy (Richter, 2018).

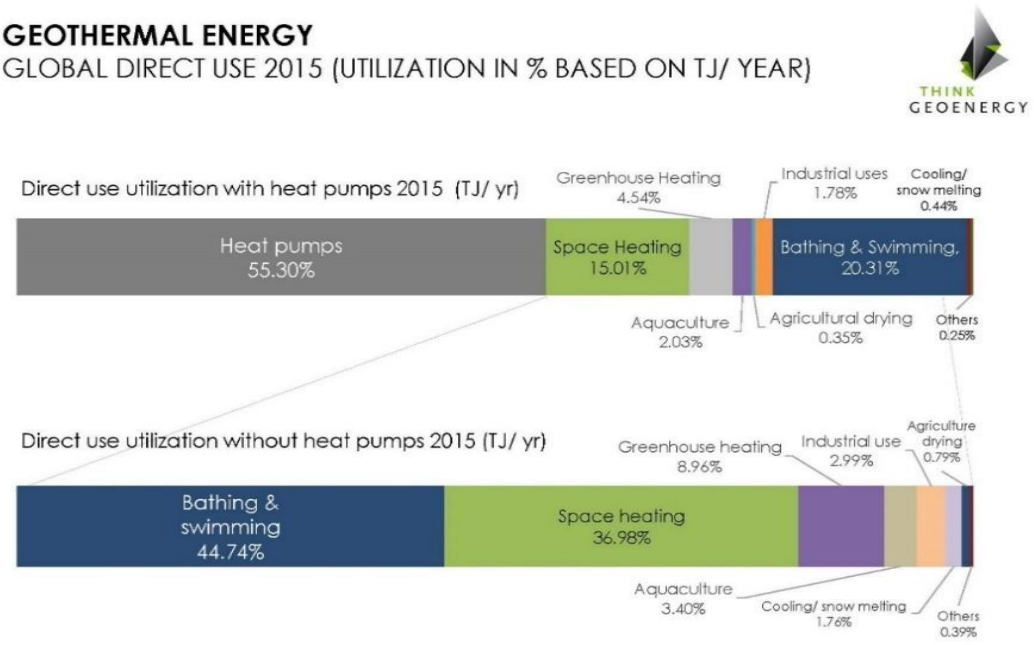

Figure 1.7 : Usage areas of geothermal energy. Adapted from Richter (2018).

Global direct use capacity is illustrated in Figure 1.8. Since 1995 there is a considerable amount of increase in heat pumps and direct use. The 2020 projection is 68000 MW_T for heat pump usage and 27000 MW_T for direct use (Richter, 2018).

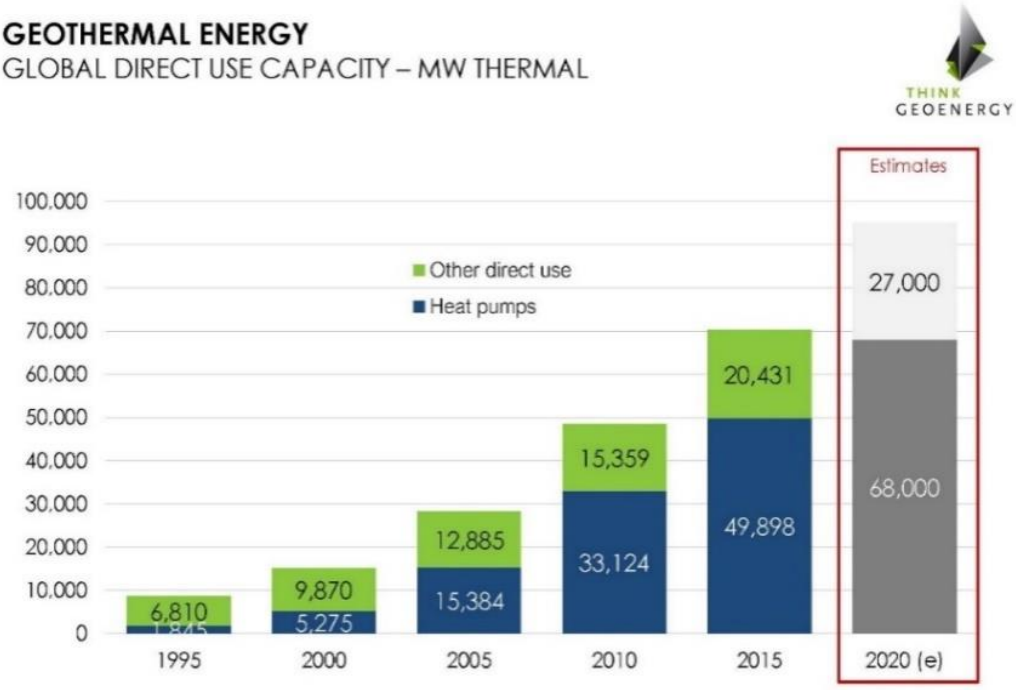

Figure 1.8 : Global Direct use capacity. Adapted from Richter (2018).

1.2 Geothermal Energy in Turkey

The use of geothermal energy started in the second half of the 1950s in Turkey. One of Turkey's vision of 2023 is to produce 30% of Turkey's electricity from renewable energy sources (Melikoglu, 2017). Turkey has available geothermal resources. Geothermal activity is common in the west of Turkey which is within Menderes Massive (Serpen et al., 2010). Figure 1.9 shows the geothermal resources map of Turkey. As seen, mainly west and central part of Turkey has geothermal activity most. Geothermal resources are classified into three groups according to fluid temperatures (Zaim and Çavşi, 2018).

- Low enthalpy areas (20^{o}C -70 ^{o}C)
- Medium enthalpy areas (70 ^{o}C - 180 ^{o}C)
- High enthalpy areas (> 180 ^{o}C)

In order to benefit from electricity production, high enthalpy areas are primarily considered, medium enthalpy areas are considered for different drying processes, greenhouse heating, and district heating, and low enthalpy areas are considered for balneotherapy uses. The use of geothermal energy depends on region conditions and fluid temperatures. In order to benefit efficiently from geothermal energy, regions closer to the geothermal source should be considered (Şimşek, 1998). Turkey has a theoretical geothermal energy potential of 31500 MW_T to 60000 MW_T, and the technical capacity that can be used is estimated as 4809 MW_T, while 2880 MW_T is the proven part of the technical capacity, 805 MW_T is used for district heating , 612 MW_T in greenhouse heating, 380 MW_T thermal facility heating, 1005 MW_T balneotherapy uses, 1.5 MW_T is used for drying of fruits, and 42.8 MW_T heat pump applications. The power production potential with the new technology and following advancements is increased to 1500 – 2000 MW_e. The power capacity of the geothermal power plants is already 1037.3 MW_e. Also, the power capacity of other geothermal power plants in construction has 230 MW_e capacity and exploitations are continuing for 650 MW_e (Kaya, 2018).

Table 1.1 shows the reservoir temperatures in the west of Turkey. Table 1.2 shows the specifications of geothermal power plants in west of Turkey.

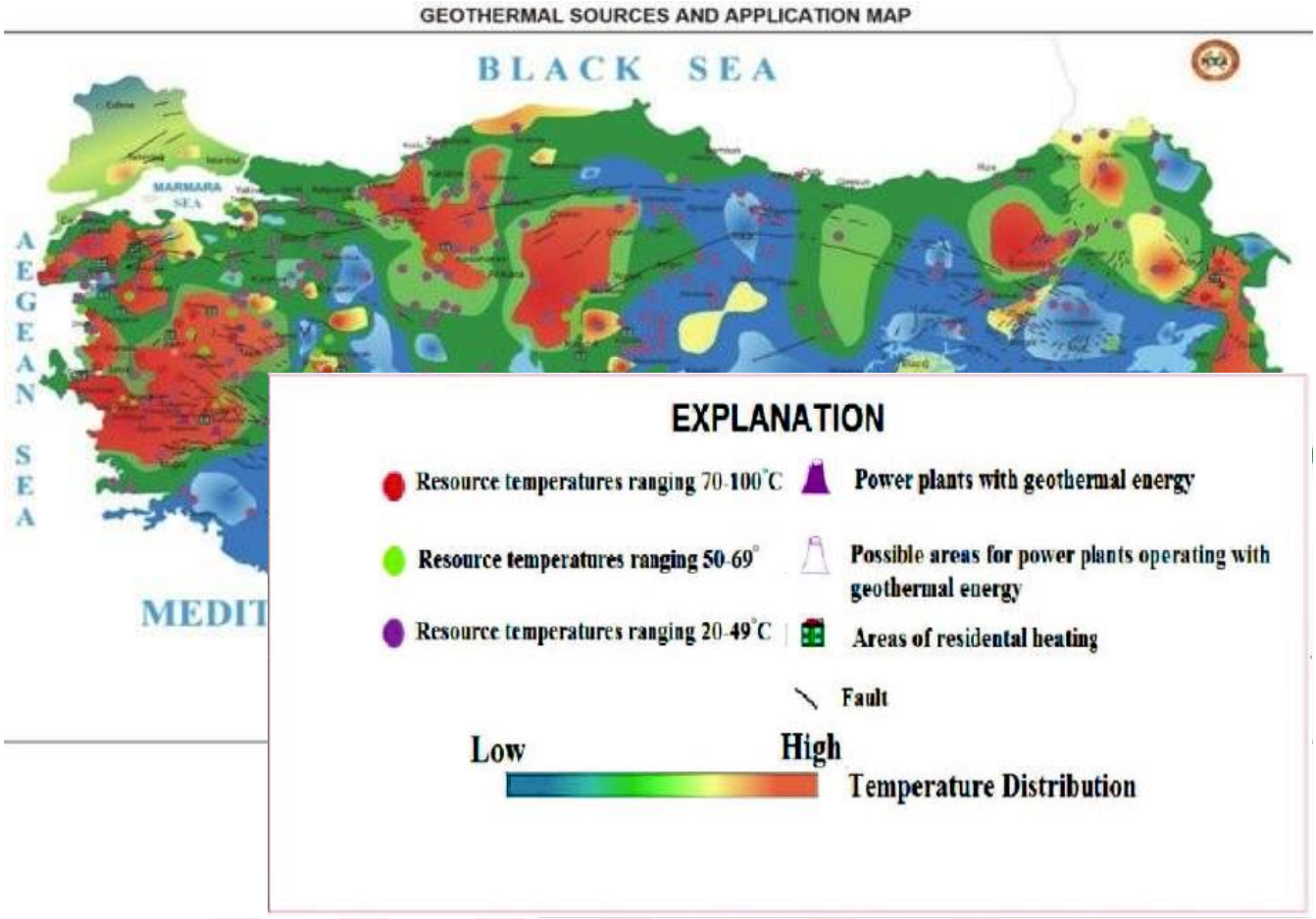

Figure 1.9 : Geothermal sources and application map of Turkey (Aksoy, 2012).

Table 1.1 : Reservoir temperatures in the west of Turkey. Adapted from Kaya (2018).

Field	Reservoir Temperatures(°C)	Field	Reservoir Temperatures(°C)
Manisa-Alaşehir-Köseali	287	Kütahya-Simav	162
Manisa Alaşehir	265	Aydın-Umurlu	155
Manisa-Alaşehir-Köseali	287	Kütahya-Simav	162
Manisa Alaşehir	265	Aydın-Umurlu	155
Manisa-Salihli-Caferbey	249	İzmir-Seferihisar	153
Denizli-Kızıldere	242	Denizli-Bölmekaya	147
Aydın-Germencik-Ömerbeyli	239	Aydın-Hıdırbeyli	146
Manisa-Alaşehir-Kurudere	214	İzmir-Dikili-H.Çiftliği	145
Aydın-Yılmazköy	192	Aydın-Sultanhisar	145
Aydın-Pamukören	188	Aydın-Bozyurt	143
Manisa-Alaşehir - Kavaklıdere	188	Denizli-Karataş	137
Manisa-Salihli-Göbekli	182	İzmir-Balçova	136
Kütahya-Şaphane	181	İzmir-Dikili-Kaynarca	130
Çanakkale-Tuzla	174	Aydın-Nazilli-Güzelköy	127
Aydın-Salavatlı	171	Aydın-Atça	124
Denizli-Tekkehamam	168	Denizli Sarayköy Gerali	114

Table 1.2 : Specifications of geothermal powerplants in west of Turkey. Adapted from Kaya (2018).

Name	Startup	Plant Type	Turbine Manufacturer	Capacity (MW_e)	Investing firm
Kızıldere 1	1984	Flash	Ansaldo	15	Zorlu Enerji
Dora-1	2006	Binary	Ormat	7,5	Mege Enerji
Dora-2	2010	Binary	Ormat	12	Mege Enerji
Gürmat-1	2009	Flash	Mitshibushi	47.4	Gürmat Elektirk
Bereket	2008	Binary	Ormat	6.5	Bereket Enerji
Enda (TJEAS)	2010	Binary	Ormat	7.5	Enda Enerji
Irem	2011	Binary	Ormat	20	Maren Enerji
Sinem	2012	Binary	Ormat	22.5	Maren Enerji
Deniz	2012	Binary	Ormat	22.5	Maren Enerji
Degirmenci	2012	Binary	Pratt&Witney	0.84	Degirmenci
Mege(Dora 3a)	2013	Binary	Ormat	21	Mege Enerji
BM	2013	Binary	Ormat	9.8	BM Enerji
Pamukören 1	2013	Binary	Atlas Copco	22.5	Çelikler Holding
Pamukören 2	2013	Binary	Atlas Copco	22.5	Çelikler Holding
Kızıldere 2	2013	Flash/Binary	Fuji+TAS	80	Zorlu Enerji
Efe 2	2014	Binary	Ormat	25	Binary Gurmat
Mege (Dora 3b)	2014	Binary	Ormat	20	Mege Enerji
Türkerler	2014	Binary	Ormat	24	Türkerler Enerji
Kerem	2014	Binary	Ormat	24	Maren Enerji
Ken	2015	Binary	Ormat	22.5	Maren Enerji
Efe 3	2015	Binary	Ormat	25	Gurmat Elektrik
Akça Enerji	2015	Binary	Exergy	3.5	Akça Enerji
Pamukören 3	2015	Binary	Atlas Copco	22.5	Çelikler Holding
Efe-4	2015	Binary	Ormat	25	Gurmat Elektrik
Efe-1	2015	Flash	Mitshibushi	47.5	Gurmat Elektrik
Karkey	2015	Binary	Exergy	12	Karadeniz Holding
MTN	2015	Binary	Atlas Copco	8	MTN Eneji
Zorlu	2015	Flash/Binary	Toshiba+TAS	45	Zorlu Enerji
Pamukören-4	2015	Binary	Atlas Copco	22.5	Çelikler Holding
Pamukören-5	2016	Binary	Atlas Copco	22.5	Çelikler Holding
Enerji Holding	2016	Binary	Exergy	24	Enerji A
Greeneco 2x12.5	2016	Binary	Exergy	25	Greeneco
Türkerler	2016	Binary	Ormat	24	Turkerler
Karkey	2016	Binary	Exergy	12	Karadeniz Holding
Mege(Dora 3a)	2016	Binary	Ormat	21	Mege Enerji
Morali	2017	Binary	Exergy	24	Karizma Enerji
Afyon	2017	Binary	Turboden-MHI	3	AFJET
Sultanhisar	2017	Binary	Atlas Copco	22	Çelikler Holding
Kizildere III U1a	2017	Flash	Toshiba	60.0	Zorlu Enerji
Kizildere III U1b	2017	Binary	Ormat	23	Zorlu Enerji
Efe 6	2017	Binary	Ormat	27	Gürmat Elektrik
TBK Kuyucak	2017	Binary	Exergy	22	Turkas
Kizildere III U2a	2017	Flash	Toshiba	52	Zorlu Enerji
Kizildere III U2b	2017	Binary	Ormat	15	Zorlu Enerji
Caferbey Salihli	2017	Binary	Ormat	16	Sanko Enerji
Total				1037.3	

Figure 1.10 and Figure 1.11 shows the growth in installed capacity in Turkey and growth of the geothermal direct use capacity in Turkey. The increase on both of the figures is caused due to the privatization moves in recent years.

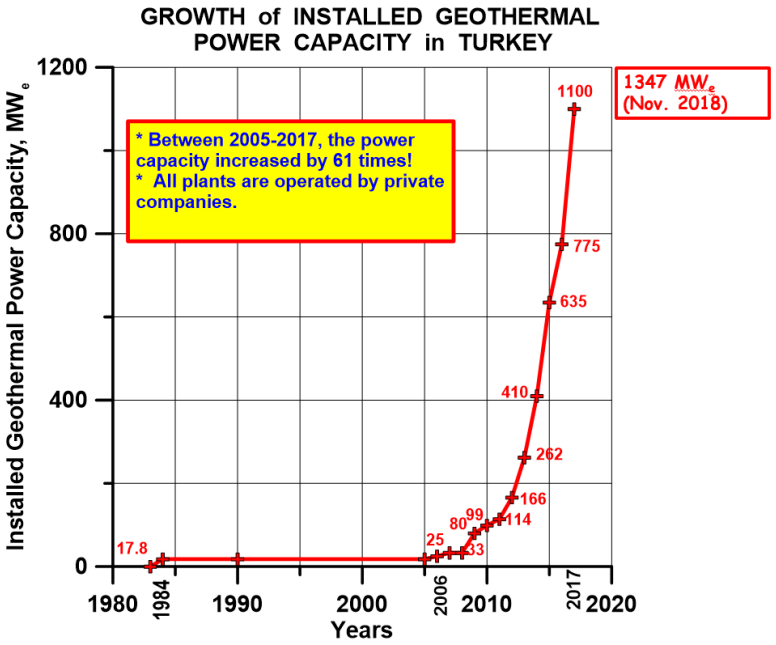

Figure 1.10 : Growth of installed geothermal power capacities in Turkey (Satman, 2018, personal communication).

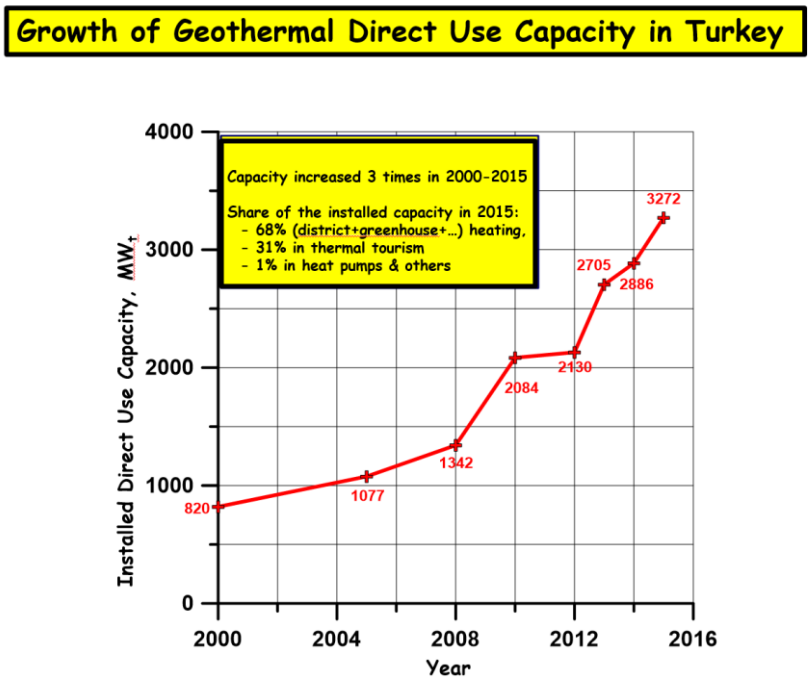

Figure 1.11 : Growth of direct geothermal use capacity in Turkey (Satman, 2018, personal communication).

1.3 Geothermal Power Plants

There are currently three types of geothermal power plants:

- Dry steam power plants
- Flash steam power plants
- Binary power plants

1.3.1 Dry steam power plants

In Figure 1.12 a dry steam power plant can be seen. In dry steam power, the reservoir consists only of steam which has a temperature between 180^{o}C - 350^{o}C. The steam can be transported by boreholes to turbines to generate electricity. There are numerous filters to remove the rock particles during transportation of steam. The first dry steam power plant was used in 1904 Lardorello Field, Italy. Also, there is another one in Geysers, California (Breeze, 2014).

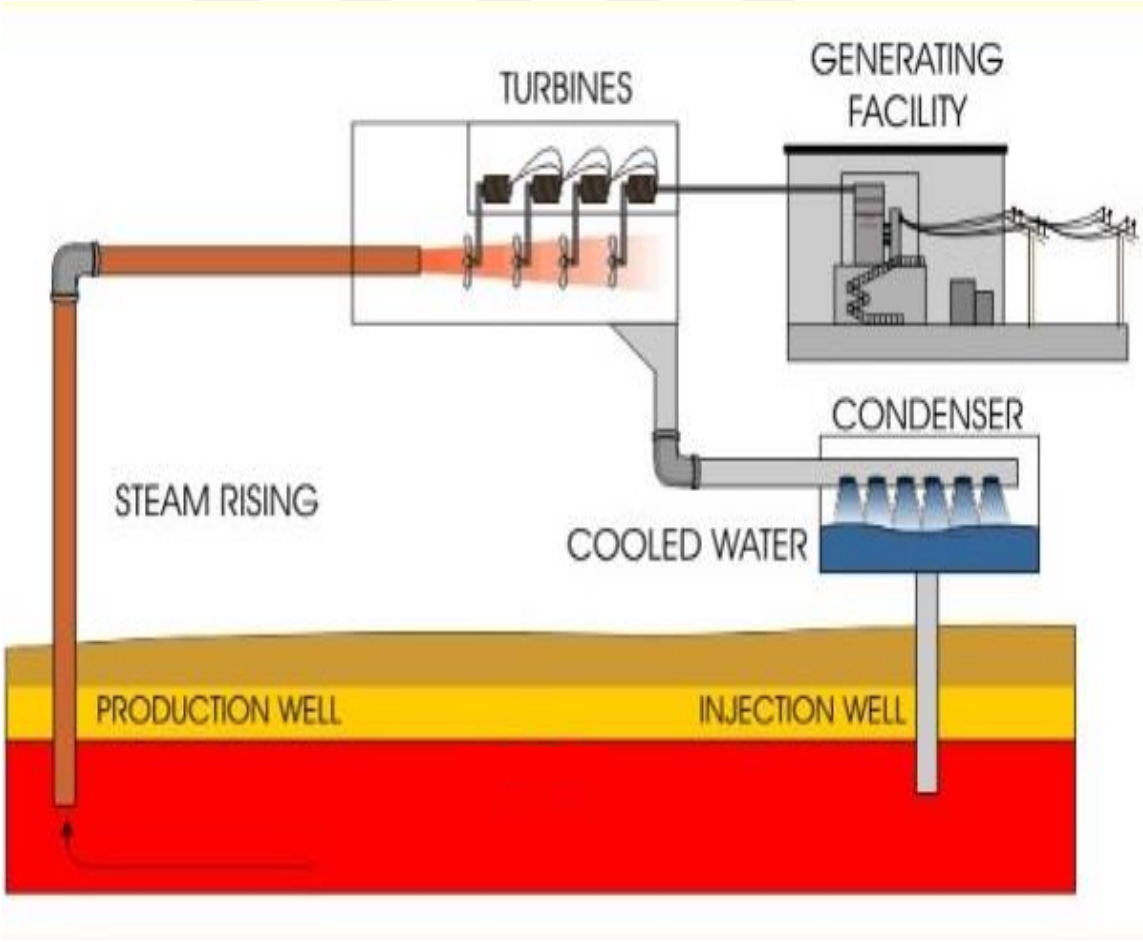

Figure 1.12 : Dry steam power plant (Url-4).

1.3.2 Flash steam power plants

In Figure 1.13 a flash steam power plant can be seen. Reservoirs which are at high temperatures may contain liquid brine and steam coexisting together. The steam is approximately 10% - 50% by weight. When the steam-water mixture is transported from the reservoir to turbines mixture has to be separated by a separator. The fluid is transported through a valve to a vessel which has a lower pressure. As a result, hot liquid flashes into steam which is then sent to the turbines. After the steam passes through the turbines, it is condensed into the water and is reinjected into the reservoir. The capacity is between 20- 55 MW_e (Breeze, 2014).

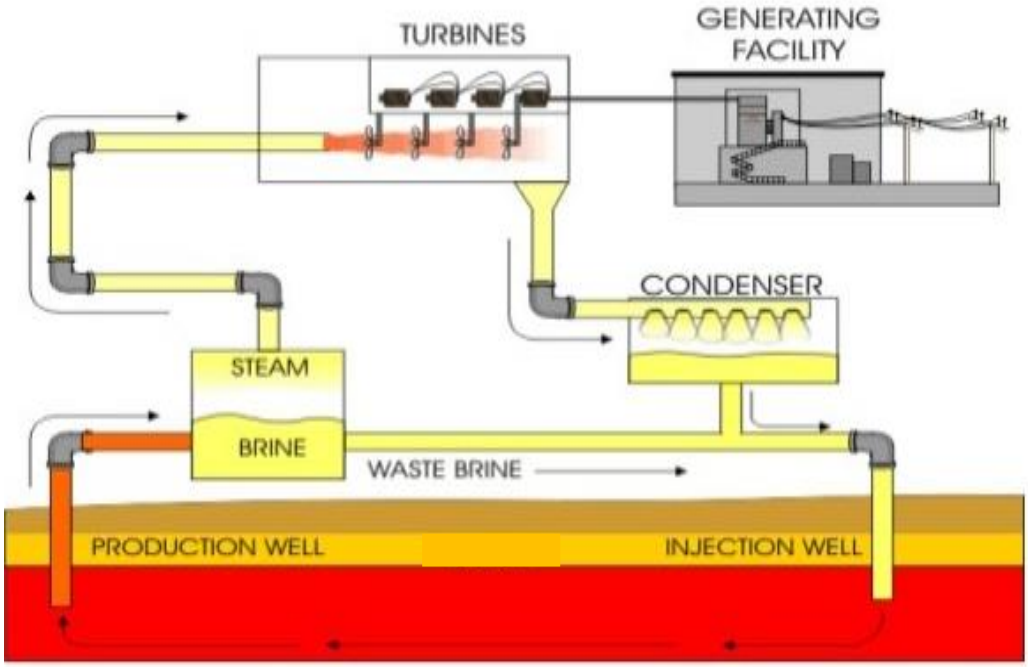

Figure 1.13 : Flash steam power plant (Url-5).

1.3.3 Binary power plants

In Figure 1.14 binary power plants can be seen. If the fluid is cooler than 180°C conventional steam technology will be too inefficient. However binary power plant can extract the energy from the ground. The main difference of this system is that the primary fluid which is extracted from the ground releases the heat within to a secondary fluid via a heat exchanger. The secondary fluid is in a closed circuit, and it is instead an organic fluid which vaporizes at low temperatures or ammonia and water mixture. The secondary fluid drives the turbines. After the turbines, the secondary fluid condenses (Breeze, 2014).

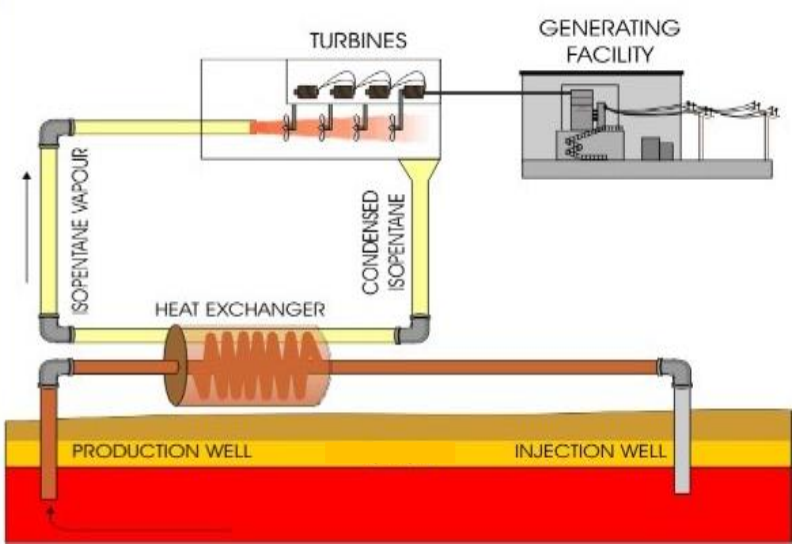

Figure 1.14 : Binary power plant (Url-6).

1.4 Geothermal Resources

Geothermal resources are classified according to gradient type, reservoir thermodynamics, and enhanced geothermal systems.

1.4.1 Geothermal resource based on gradient type

Convective and conductive systems are two main categories which temperature gradient can be separated. Figure 1.15 shows the difference between conductive and convective system. In conductive systems, temperature increases linearly with depth due to the upward heat flow. In a convective system temperature remains constant with depth also contains both liquid and vapor. Enhanced geothermal systems(EGS) can be an example of a conductive system.

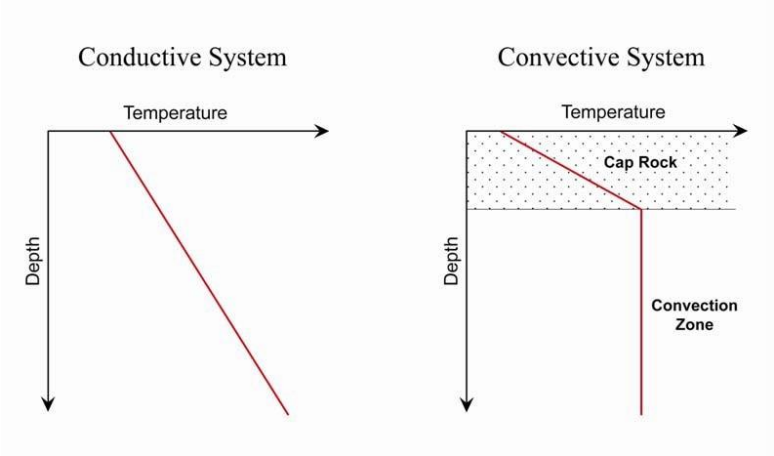

Figure 1.15 : Conductive and convective systems (Sanyal, 2010).

1.4.2 Geothermal resource based on reservoir thermodynamics

The physical states are the primary object when categorizing a reservoir. A reservoir can be liquid dominated, vapor-dominated or in some case it may contains 2 phases. In liquid dominated reservoirs water is at temperatures below or at boiling. In vapor-dominated systems, the temperature is above the boiling point temperature. In two-phase systems, the temperature is at boiling point.

1.4.3 Enhanced geothermal systems

An Enhanced geothermal system (EGS) can be created when there is insufficient fluid saturation or permeability. It can also be defined as an artificial human made reservoir. In an EGS, injection of fluid into the reservoir causes fractures and creates an increase in permeability. When permeability increases, it allows fluid to circulate throughout the newly fractured rock and to transport heat to the surface where electricity can be generated (U.S Department of Energy, 2016). EGS system can be seen in Figure 1.16.

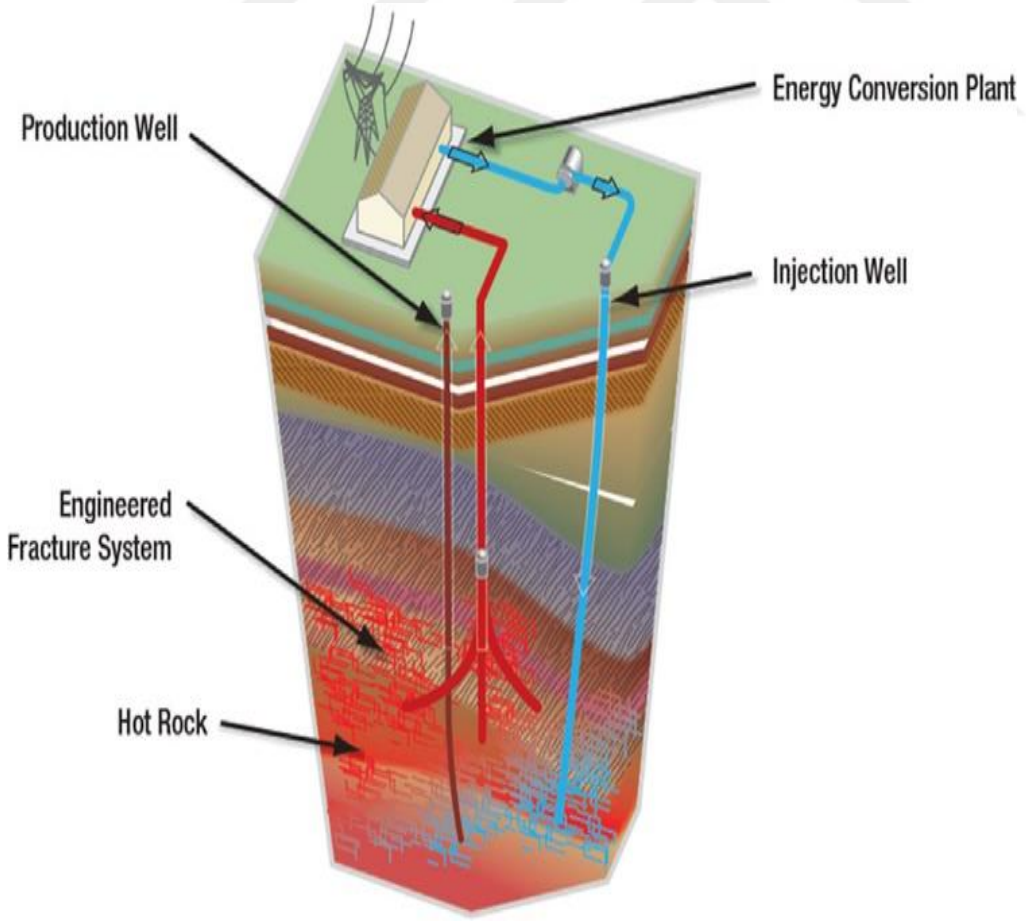

Figure 1.16 : Enhanced geothermal system (Olasolo et al., 2016).

1.5 Effects of CO_2 in Geothermal Reservoirs

For evaluation of geothermal fields and for the prediction of future performances geothermal reservoir simulation is a must. In the early years of reservoir simulations the content of geothermal fluid was considered to be only water; however, NCGs such as CO_2 can also exist in the geothermal fluid. In the west of Turkey most of the reservoir fluids contain a high amount of NCGs. The NCG gas is 96% to 98% CO_2 and is dissolved between 200°C±50°C in liquid-dominated reservoirs (Haizlip et al., 2016). For example in the Kızıldere field which is located in Denizli, the reservoir contains 1.5% to 3% of CO_2 (Satman et al., 2005). Also, Germencik field and Ömer – Gecek field contains 2.1% and 0.4% of CO_2 respectively (Satman et al., 2007). In order to understand the effect of CO_2 in geothermal reservoirs, Figure 1.17 is given. In Figure 1.17, the pressure-temperature graph of water for different amounts of CO_2 fractions is given. As it is clear from Figure 1.17, the main effect of CO_2 content is that it causes a considerable increase in the flashing point of the fluid. This effect is most profound between 350 K- 500 K. For example at 375 K for a fraction of 0.5% CO_2, the pressure is around 1.6 Mpa, whereas for a fraction of 2.5% the pressure is around 8.4 Mpa. Moreover, for higher temperatures like 600 K, for a fraction of 0.5%, the pressure is about 15 Mpa, whereas for a fraction of 2.5% the pressure is around 17 Mpa.

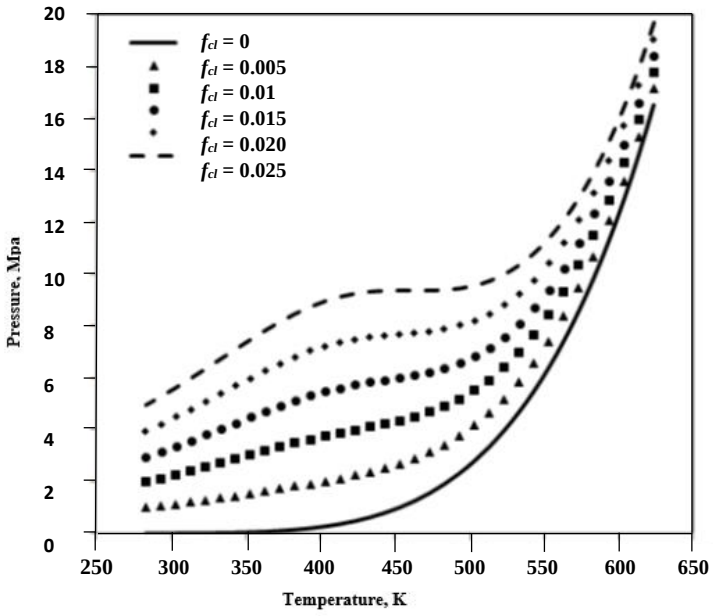

Figure 1.17 : Temperature - pressure diagram of CO_2 adapted from Hoşgör et al. (2015).

The partial pressure of CO_2 is higher than the vapor pressure. As a result, flashing occurs at higher pressures (Kaya et al., 2005). Figure 1.18 shows how the partial pressure of CO_2 changes with different fractions of CO_2 and with temperature.

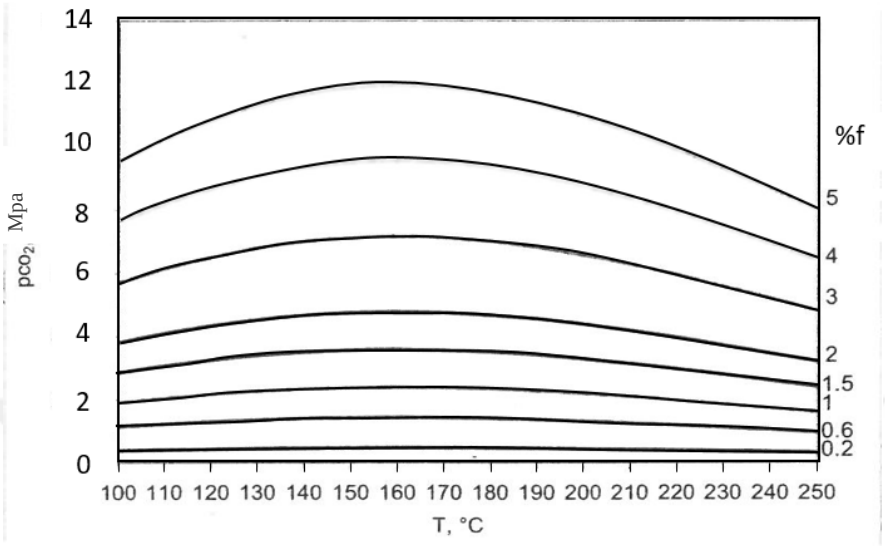

Figure 1.18 : Change of partial pressure of CO_2. Adapted from Kaya et al. (2005).

Figure 1.19 illustrates how the flashing point in well changes during production. It is clear from Figure 1.19, as the CO_2 content is increased, the flashing point in the well is observed at greater depths. This results in higher wellhead pressures. As a result the high wellhead pressures are again caused by the much higher partial pressure of CO_2.

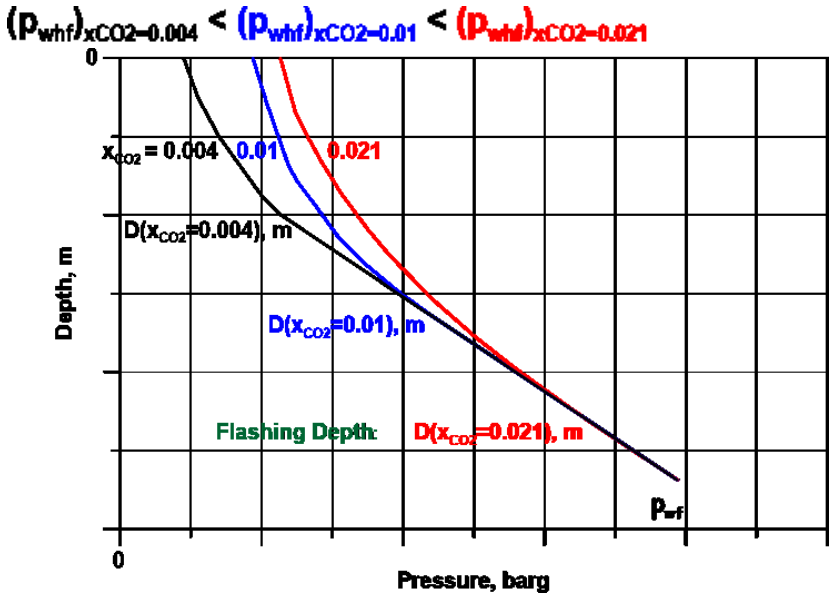

Figure 1.19 : Wellhead pressure profile (Satman et al., 2017).

1.6 Literature Review

To have a better understanding of geothermal systems, geothermal reservoir modeling is crucial. In geothermal reservoir modeling, the physical properties of the reservoir should be obtained and understood clearly. This also is related to the management of the resource or reservoir. After getting complete information about the reservoir then future performance predictions are made for specifying how much a reservoir is going to be used and also gives a good idea of estimation of potential. Geothermal reservoir engineering deals with heat transfer, transportation of fluid and chemical reactions (Donaldson et al., 1983). Initially, a volumetric method is used for estimating the heat in place in which porosity, depth, area and fluid properties are used. However further modeling is necessary through integration of production data. Reservoirs can be modeled in three ways: Decline curve method, numerical simulation, and lumped parameter modeling. In decline curve method an equation is fitted into flow rate decline data which is obtained from wells. However, sufficient data must be obtained, and changes in the field operation are not taken into account (Bodvarsson et al., 1986). The use of harmonic, exponential and logarithmic functions to curve fit data have been suggested in the literature by Arps (1945) and Chierici (1964). An example of the use of decline curve could be the Lardorello field which is in Italy and the Geysers field which is in California (Budd, 1972; Stockton et al., 1984). In numerical simulations, the geothermal reservoir is divided into grid blocks and conservation equations are applied to each grid block simultaneously. With the help of the computer, nonlinear partial differential equations are solved. This method is mostly used when there is petrophysical and production data. The disadvantage of the numerical modeling is that it may be very time-consuming especially when history matching to production data is involved. However, lumped parameter modeling, provide faster run times and require fewer data. Lumped parameter method is a type of simplified version when compared with the numerical method. Discussed above in numerical method grid blocks exists, in lumped parameter modeling only one or more homogenous tanks which are assumed to be composed of fluid and rock is utilized (Sarak et al., 2005). Tanks which have physical reservoir parameters represents the reservoir, heat source, aquifer or the place which natural discharge occurs.

1.6.1 Lumped parameter models

Whiting and Ramey Jr (1969) and Brigham and Ramey Jr (1981) introduced a lumped parameter model which included material and energy balances. Including the physical reservoir parameters such as porosity, density, bulk volume, pressure, and temperature. For different geometries, water influx models were used. The equations can give information about the initial condition of the reservoir, history matching and future performance predictions of the reservoir can be modeled.

Sanyal et al. (1976) suggested an analytical approach for heat transfer and the fluid flow in hot water reservoir. A multilayered reservoir which consists of circular injection and production wells were observed. Rock properties can vary through layers and flow at steady state is assumed. For the heat transfer problem, Gringarten and Sauty (1975) approach are used. Moreover, the results were very close to the numerical ones when it was applied to the Heber geothermal reservoir in the Imperial Valley, California.

Grant (1977) incorporated CO_2 in a lumped parameter model of Ohaki-Broadlands reservoir which is a hot water system containing few percents of carbon dioxide. The study showed that the partial pressure of CO_2 caused pressure drops at early times.

Atkinson et al. (1980) modeled the Bagnore field, which is a vapor-dominated reservoir, containing few amounts of CO_2, with lumped parameter modeling. Since the reservoir was in two-phase, Two tank modeling was used in the study by the authors, one tank for modeling the liquid region and the other tank for the vapor region.

Castanier et al. (1980) and, Castanier and Brigham (1983) introduced a model which can be applied to steam dominated, liquid dominated and two-phase geothermal reservoirs.

Olsen (1984) and Gudmundsson and Olsen (1987) represented a depletion model for liquid-dominated geothermal reservoirs. Including water flux depletion models for recharge and no recharge were used and applied to one of the high-temperature geothermal fields in Svartsenghi, Iceland.

Axelsson (1985) used simple lumped parameters in the simulation of long-term production only for drawdown and production data. The analytical response was also obtained for real systems.

Axelsson (1989) and Axelsson and Dong (1998) and Axelsson and Gunnlaugsson (2000) represented a lumped parameter method that simulates data from low-temperature geothermal fields in Iceland.

Alkan and Satman (1990) introduced a thermodynamical package which described the behavior of water CO_2 systems. This model could be used for liquid dominated system and pressurized water CO_2 system. The model was tested in Ohaaki, Cerro Prieto, Kızıldere and Bagnore fields.

Later for low-temperature fields another model is introduced by Sarak et al. (2005). The behavior of low-temperature geothermal reservoirs was analytically simulated. Parameters were obtained for two fields by way of history matching.

A new non-isothermal lumped parameter model for low-temperature liquid dominated reservoirs was introduced by Onur et al. (2008) who developed a new generalized non-isothermal lumped parameter model used in the prediction of temperature and pressure behavior of geothermal reservoirs.

Tureyen et al. (2009) developed a generalized lumped parameter model that links the system to multiple tanks such as aquifers and multiple reservoirs and enables the variation of temperature and pressure effects. Later Tureyen and Akyapı (2011) developed the studies of Onur et al. (2008) and Tureyen et al. (2009) by adding conduction effect into the system.

Later Hosgor et al. (2016) developed a model to investigate the geothermal reservoirs with CO_2 content. The change in pressure and temperature due to recharge, reinjection and production; furthermore change of gas saturation of the reservoir could be calculated with the developed model.

1.7 Purpose of the Thesis

In this study, a model is developed for keeping track of the carbon dioxide content of a geothermal reservoir. The model consists of solving the lumped parameter model numerically that gives CO_2 content as a function of time. The developed model is a

lumped parameter model for liquid-dominated geothermal reservoirs and is capable of working with multiple tanks. In the next Chapter, the details of the model are presented along with the verifications with an existing model in the literature. This is followed in Chapter 3 by various applications where production/reinjection strategies are shown. The thesis ends with Conclusions.

2. MATHEMATICAL MODEL

In this section, the details of the mathematical model developed in this study is given. However, before the model is introduced first the analytical model of Hosgor et al. (2016) is provided. This analytical model will serve as a benchmark for the verifications of the model developed in this study.

2.1 Analytical Models

The model of Hosgor et al. (2016) which is used in this thesis for verification purposes, is a lumped parameter model, and the developed model aims to give the amount of change of the CO_2 content in the reservoir due to production, injection, and recharge in liquid-dominated reservoirs. This model is for a single tank only and gives the analytical expression for the change at the CO_2 content. Mass balance application of CO_2 over any control volume is the basis of the model. The schematics of the model is provided in Figure 2.1. There are mainly three sources of CO_2, which are from production, injection and natural recharge. w_{inj} is the mass injection rate of water, and w_p is the production mass rate, w_{re} is the natural recharge mass rate. The mass fraction of CO_2 is shown with f, reinjection mass fraction rate is shown with f_{inj}, and mass fraction rate of CO_2 due to recharge is shown with f_{re} (Hosgor et al., 2016).

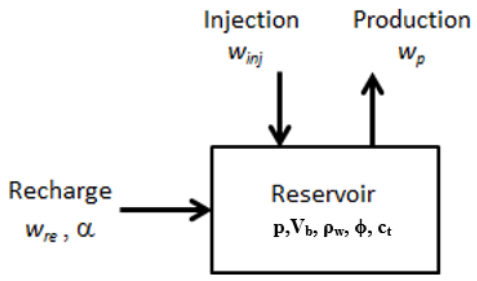

Figure 2.1 : Diagram of water accumulation (Hosgor et al., 2016).

According to Hosgor et al. (2016), the general equation for mass balance is shown in Equation 2.1. Generally, accumulation rate of CO_2 is equal to injected CO_2 mass rate, the mass rate of CO_2 from natural recharge and production rate of CO_2.

The mass balance equation for the model is shown in Equation 2.1 :

$$\begin{aligned}&\text{Accumulation Rate of } CO_2 = \text{Injected } CO_2 \text{ mass rate} \\ &+ \text{Mass rate of } CO_2 \text{ from natural recharge} - \text{Produced } CO_2 \text{ mass rate}\end{aligned} \tag{2.1}$$

Mathematically Equation 2.1 can be expressed as follows :

$$\frac{dm}{dt} = w_{inj} f_{inj} + w_{re}(t) f_{re} - w_p f(t) \tag{2.2}$$

The mass of CO_2 is shown by m (kg), time is shown as t (s). CO_2 mass fraction is shown by f (t). The mass rates are represented by w (kg/s) where w_{inj} (kg/s) is the mass injection rate, w_{re} (kg/s) is mass recharge rate and w_p (kg/s) is the production rate. Here w_p and w_{inj} are treated as constant; also the subscripts *inj*, *re* and *p* refers to the injection, recharge, and production rates respectively. Recharge mass rate is shown as a function of time. To note; reinjection and recharge mass fractions of CO_2 are constant. The mass of CO_2 in the reservoir can be expressed as shown in the Equation. 2.3:

$$\frac{d\left[V_b \phi \rho_w f(t)\right]}{dt} = w_{inj} f_{inj} + w_{re}(t) f_{re} - w_p f(t) \tag{2.3}$$

For simplicity, it is assumed that the bulk volume, porosity and density are more or less constant which leads to the Equation. 2.4 :

$$V_b \phi \rho_w \frac{df(t)}{dt} = w_{inj} f_{inj} + w_{re}(t) f_{re} - w_p f(t) \tag{2.4}$$

According to Hosgor et al. (2016) Equation, 2.4 can be written as Equation 2.5 through the use of storage capacity :

$$\frac{\kappa}{c_t} \frac{df(t)}{dt} = w_{inj} f_{inj} + w_{re}(t) f_{re} - w_p f(t) \tag{2.5}$$

The storage capacity is denoted by κ (kg/bar):

$$\kappa = V_b \phi \rho_w c_t \tag{2.6}$$

Here c_t is the total compressibility (1/bar). For modeling the recharge rate w_{re} as a function of time the Schilthuis (1936) relation is used which is shown in Equation 2.7:

$$w_{re} = \alpha(p_0 - p(t)) \tag{2.7}$$

p_0 is the initial pressure, and it is constant in Equation 2.7. According to Hosgor et al. (2016) Equation 2.7 can be written as Equation 2.8:

$$w_{re} = \alpha(\Delta p(t)) \tag{2.8}$$

If Equation 2.8 is integrated into Equation 2.5, then Equation 2.9 is obtained.

$$\frac{\kappa}{c_t}\frac{df(t)}{dt} = w_{inj} f_{inj} + \alpha \Delta p(t) f_{re} - w_p f(t) \tag{2.9}$$

In Equation 2.9 there is α which symbolizes recharge constant (kg/bar.s). The pressure drop is denoted by Δp (bar).

The solution of Δp (t) in Equation 2.9 is provided by Sarak et al. (2005) and is given in Equation 2.10:

$$\frac{\kappa}{c_t}\frac{df(t)}{dt} + w_p f(t) - (w_{inj} f_{inj} + w_n f_{re}) + w_n f_{re} e^{\frac{-\alpha t}{\kappa}} = 0 \tag{2.10}$$

Inserting Equation 2.10 into Equation 2.9 will result in Equation 2.11:

$$\Delta p(t) = \frac{w_n}{\alpha}\left[1 - e^{\frac{\alpha t}{\kappa}}\right] \tag{2.11}$$

For the ODE, given in Equation 2.11 initial condition is given in Equation 2.12 :

$$f(t=0) = f_0 \tag{2.12}$$

According to Hosgor et al. (2016) the solution of Equation 2.11 is given as Equation 2.13:

$$f(t) = f_0 e^{-\left(\frac{W_p c_t}{\kappa} t\right)} + \frac{w_{inj} f_{inj} + w_n f_{re}}{w_p} + \frac{w_n f_{re}}{w_p - \frac{\alpha}{c_t}} e^{-\left(\frac{W_p c_t}{\kappa} t\right)} - \frac{w_n f_{re}}{w_p - \frac{\alpha}{c_t}} e^{-\left(\frac{\alpha}{\kappa} t\right)} + \frac{w_{inj} f_{inj} + w_n f_{re}}{w_p} e^{-\left(\frac{w_p c_t}{\kappa} t\right)} \quad (2.13)$$

Equation 2.13 provides the change in carbon dioxide as a function of time. For the investigation of the system in a steady state, a modification is required, that is; when term *t* goes to infinity only one steady state term will remain, which is provided in Equation 2.14. According to Equation 2.14, when the system is at steady state, only w_{inj}, f_{inj}, $w_n f_{\text{re}}$ and w_p, parameters will affect the steady state CO_2 content.

$$f(t) = \frac{w_{inj} f_{inj} + w_n f_{re}}{w_p} \quad (2.14)$$

2.2 Multi Tank Model

In this section, the construction of the numerical solution of the lumped parameter model, and the solution methodology is given. Figure 2.2, gives the schematics of any tank *i*, making an arbitrary number of connections to neighboring tanks. Three conservation equations are written for tank *i*; mass balance on liquid water, mass balance on carbon dioxide and an overall energy balance.

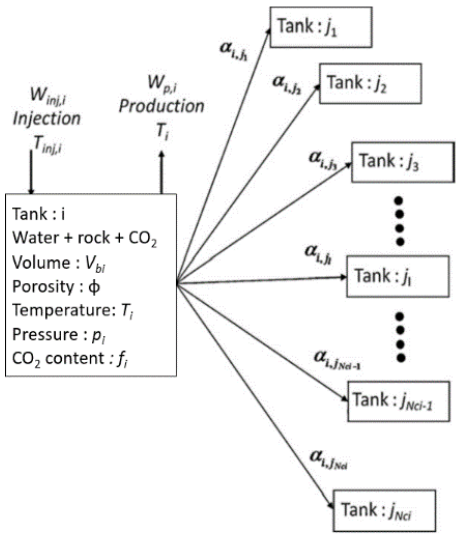

Figure 2.2 : Tank connections, neighboring tanks and the properties of them.

Physical reservoir parameters of the tank, that is composed of rock and fluid are shown in Figure 2.2. V_{bi} (m^3) is the bulk volume of the tank *i*, porosity of the tank *i* is denoted by ϕ_i, the temperature at tank *i* is T_i (°C), the pressure is p_i, (bar). Any tank *i*, for i=1,2,..., N_t, can make connections with any other tank j_l in the model. N_{ci} is the total number of connections of tank *i* and any other connecting tank to the system will be represented by j_l in which l=1,2,…, N_{ci} , and f_i is the mass fraction of CO_2 for tank *i*. The injection term with a specified mass rate of the tank *i* is $w_{inj,i}$ (kg/s), and the injection temperature will be denoted by $T_{inj,i}$ (°C). The production term is denoted by a mass rate of $w_{p,i}$ (kg/s), and the mass recharge rate is shown by w_{re} (kg/s), and the producing reservoir fluid temperature is T_i (°C).

2.2.1 Mass balance for water

The mass rate of the recharge source which is shown by w_{re} (kg/s), to the tank *i* could be modeled with Schilthuis (1936) relationship given in Equation 2.15.

$$\mathrm{w}_{\mathrm{re}} = \alpha_{re}(p_i - p_l) \tag{2.15}$$

Hence the mass balance equation for tank *i* is given in Equation 2.16 :

$$V_{bi}\frac{d(\rho_{w,i}\phi_i)}{dt} - \sum_{l=1}^{N_{ci}} \alpha_{i,j_l}(p_{j_l} - p_i) + \left[w_{p,i} + w_{inj,i}\right] = 0 = \mathbf{r}_W \tag{2.16}$$

The density of the water in any tank *i* is represented by $\rho_{w,i}$. Accumulation of the reservoir, the mass flow rate from the recharge source, the net flow rate from the tanks and net production rate from the tanks are represented in the left-hand side of the Equation 2.16. Here **r** represent the residual.

2.2.2 Overall energy balance

The energy balance equation is set up in such a way that both convective and conductive heat transfer between the tanks is taken into consideration. Fluid movement because of recharge, production or injection causes a change in temperature. Heat transfer by way of conduction is modeled as follows, which is shown in Equation 2.17:

$$Q = \gamma_{i,jl}(T_{jl} - T_i) \tag{2.17}$$

Here Q is the energy rate (J/s), heat conductance between the tanks is represented by $\gamma_{i,jl}$. (J/ K.s). Conservation of energy shown in Equation 2.18 is as follows:

$$\begin{aligned} &\frac{d}{dt}\left[(1-\phi)V_b\rho_m C_m T + V_b\phi\rho_w u_w\right] + w_{inj,i}h_{w,inj,i} + w_p h_{w,i} \\ &-\sum_{l=1}^{N_{ci}}\alpha_{i,jl}(p_{jl} - p_i)h_\xi - \sum_{l=1}^{N_{ci}}\gamma_{i,jl}(T_{jl} - T_i) = 0 = \mathbf{r}_E \end{aligned} \tag{2.18}$$

In Equation 2.18 ρ_m (kg/m^3) represents the density of the rock matrix, C_m (J/(kg. K)) represents the specific heat capacity of the rock matrix, u (J/kg) represents the internal energy and h (J/kg) represents the enthalpy.

Using an upwinding approach for the enthalpy of water is necessary for this system which is shown in Equation 2.19:

$$h_\xi = \begin{Bmatrix} h_{w,i}, p_i \rangle p_{jl} \\ h_{w,jl}, p_i \langle p_{jl} \end{Bmatrix} \tag{2.19}$$

The Equation for the change of porosity with respect to pressure and temperature is given in Equation 2.20 as follows:

$$\phi(p,t) = \phi_0\left[1 + c_r(p - p_0) - \varepsilon(T - T_0)\right] \tag{2.20}$$

ϕ_0 is the porosity of the tank at initial conditions, c_r (1/bar) is the compressibility of the rock, and ε (1/°C) is the thermal expansivity of the rock (Onur et al., 2008).

2.2.3 Mass balance for carbon dioxide

The mass balance for carbon dioxide content is given as the following equation:

$$V_{bi}\frac{d(\rho_{w,i}\phi_i f_i)}{dt} - \sum_{l=1}^{N_{ci}}\alpha_{i,j_l}(p_{j_l} - p_i)f_\xi + \left[w_{p,i}f_i + w_{inj,i}f_{inj,i}\right] = 0 = \mathbf{r}_{WC} \tag{2.21}$$

In Equation 2.21, there are three different terms in comparison to Equation 2.16. $_{f,i}$ is the mass fraction of the CO_2 in the tank at any time, f_ξ is the contribution from connecting tanks CO_2 mass fraction, and $f_{inj,\,i}$ is the reinjection CO_2 mass fraction at any tank i.

An upwinding approach is also used for the CO_2 mass fraction which is shown in Equation 2.22. It is important to note that the model currently does not take into account the diffusion of CO_2 between the tanks. CO_2 contribution due to concentration difference is not taken into account.

$$f_{\xi} = \begin{cases} f_{w,i}, p_i \rangle p_{jl} \\ f_{w,jl}, p_i \langle p_{jl} \end{cases} \tag{2.22}$$

2.2.4 Methodology

In the numerical solution of the lumped parameter model, all of the three mass balance equation sets are solved simultaneously using a fully implicit scheme. The fully implicit scheme introduces a nonlinearity. The nonlinearity is handled by the Newton - Raphson method. An equation of how the Newton - Raphson method work is shown in Equation 2.23:

$$\underline{\underline{\mathbf{J}}}.\underline{\delta} = -\mathbf{r} \tag{2.23}$$

Here J represents the Jacobian matrix, δ represents the difference in the solution vector and r represents the vector of residuals. Below is an example for a system of a total of N_t number of tanks. In Jacobian matrix subscripts *E, W, WC* describes energy balance, mass balance on water, and mass balance on CO_2 content. Newton - Raphson technique is used in the solving of the equation systems. The Jacobian matrix, is shown in Equation 2.24.

$$\underline{\underline{\mathrm{J}}} = \begin{bmatrix} \frac{\partial \mathrm{r}_{W,1}}{\partial p_1} & \frac{\partial \mathrm{r}_{W,1}}{\partial T_1} & \frac{\partial \mathrm{r}_{W,1}}{\partial f_1} & \frac{\partial \mathrm{r}_{W,1}}{\partial p_2} & \frac{\partial \mathrm{r}_{W,1}}{\partial T_2} & \frac{\partial \mathrm{r}_{W,1}}{\partial f_2} & \cdots & \frac{\partial \mathrm{r}_{W,1}}{\partial p_{N_t}} & \frac{\partial \mathrm{r}_{W,1}}{\partial T_{N_t}} & \frac{\partial \mathrm{r}_{W,1}}{\partial f_{N_t}} \\ \frac{\partial \mathrm{r}_{E,1}}{\partial p_1} & \frac{\partial \mathrm{r}_{E,1}}{\partial T_1} & \frac{\partial \mathrm{r}_{E,1}}{\partial f_1} & \frac{\partial \mathrm{r}_{E,1}}{\partial p_2} & \frac{\partial \mathrm{r}_{E,1}}{\partial T_2} & \frac{\partial \mathrm{r}_{E,1}}{\partial f_2} & \cdots & \frac{\partial \mathrm{r}_{E,1}}{\partial p_{N_t}} & \frac{\partial \mathrm{r}_{E,1}}{\partial T_{N_t}} & \frac{\partial \mathrm{r}_{E,1}}{\partial f_{N_t}} \\ \frac{\partial \mathrm{r}_{WC,1}}{\partial p_1} & \frac{\partial \mathrm{r}_{WC,1}}{\partial T_1} & \frac{\partial \mathrm{r}_{WC,1}}{\partial f_1} & \frac{\partial \mathrm{r}_{WC,1}}{\partial p_2} & \frac{\partial \mathrm{r}_{WC,1}}{\partial T_2} & \frac{\partial \mathrm{r}_{WC,1}}{\partial f_2} & \cdots & \frac{\partial \mathrm{r}_{WC,1}}{\partial p_{N_t}} & \frac{\partial \mathrm{r}_{WC,1}}{\partial T_{N_t}} & \frac{\partial \mathrm{r}_{WC,1}}{\partial f_{N_t}} \\ \vdots & \vdots & \vdots & \vdots & \vdots & \vdots & \cdots & \vdots & \vdots & \vdots \\ \vdots & \vdots & \vdots & \vdots & \vdots & \vdots & \cdots & \vdots & \vdots & \vdots \\ \vdots & \vdots & \vdots & \vdots & \vdots & \vdots & \cdots & \vdots & \vdots & \vdots \\ \vdots & \vdots & \vdots & \vdots & \vdots & \vdots & \cdots & \vdots & \vdots & \vdots \\ \vdots & \vdots & \vdots & \vdots & \vdots & \vdots & \cdots & \vdots & \vdots & \vdots \\ \frac{\partial \mathrm{r}_{W,N_t}}{\partial p_1} & \frac{\partial \mathrm{r}_{W,N_t}}{\partial T_1} & \frac{\partial \mathrm{r}_{W,N_t}}{\partial f_1} & \frac{\partial \mathrm{r}_{W,N_t}}{\partial p_2} & \frac{\partial \mathrm{r}_{W,N_t}}{\partial T_2} & \frac{\partial \mathrm{r}_{W,N_t}}{\partial f_2} & \cdots & \frac{\partial \mathrm{r}_{W,N_t}}{\partial p_{N_t}} & \frac{\partial \mathrm{r}_{W,N_t}}{\partial T_{N_t}} & \frac{\partial \mathrm{r}_{W,N_t}}{\partial f_{N_t}} \\ \frac{\partial \mathrm{r}_{E,N_t}}{\partial p_1} & \frac{\partial \mathrm{r}_{E,N_t}}{\partial T_1} & \frac{\partial \mathrm{r}_{E,N_t}}{\partial f_1} & \frac{\partial \mathrm{r}_{E,N_t}}{\partial p_2} & \frac{\partial \mathrm{r}_{E,N_t}}{\partial T_2} & \frac{\partial \mathrm{r}_{E,N_t}}{\partial f_2} & \cdots & \frac{\partial \mathrm{r}_{E,N_t}}{\partial p_{N_t}} & \frac{\partial \mathrm{r}_{E,N_t}}{\partial T_{N_t}} & \frac{\partial \mathrm{r}_{E,N_t}}{\partial f_{N_t}} \\ \frac{\partial \mathrm{r}_{WC,N_t}}{\partial p_1} & \frac{\partial \mathrm{r}_{WC,N_t}}{\partial T_1} & \frac{\partial \mathrm{r}_{WC,N_t}}{\partial f_1} & \frac{\partial \mathrm{r}_{WC,N_t}}{\partial p_2} & \frac{\partial \mathrm{r}_{WC,N_t}}{\partial T_2} & \frac{\partial \mathrm{r}_{WC,N_t}}{\partial f_2} & \cdots & \frac{\partial \mathrm{r}_{WC,N_t}}{\partial p_{N_t}} & \frac{\partial \mathrm{r}_{WC,N_t}}{\partial T_{N_t}} & \frac{\partial \mathrm{r}_{WC,N_t}}{\partial f_{N_t}} \end{bmatrix} \tag{2.24}$$

δ vector is shown in Equation 2.25:

$$\underline{\delta} = \begin{bmatrix} \delta_{p_1} \\ \delta_{T_1} \\ \delta_{f_1} \\ . \\ . \\ . \\ . \\ . \\ . \\ \delta_{p,N_T} \\ \delta_{T,N_T} \\ \delta_{f,N_T} \end{bmatrix} \tag{2.25}$$

-r vector is shown in Equation 2.26:

$$-\mathbf{r} = \begin{bmatrix} -\mathbf{r}_{W,1} \\ -\mathbf{r}_{E,1} \\ -\mathbf{r}_{WC,1} \\ . \\ . \\ . \\ . \\ . \\ . \\ -\mathbf{r}_{W,N_T} \\ -\mathbf{r}_{E,N_T} \\ -\mathbf{r}_{WC,N_T} \end{bmatrix} \tag{2.26}$$

2.3 Verification of the Model

In this section, the verification of the numerical solution of the lumped parameter model of a single tank system is given. The analytical expression is given in Equation 2.13, and the numerical expression is the numerical solution of the analytical model. The model parameters used in the verification example are given in Table 2.1.

Table 2.1 : Parameters used in the verification of the model.

Parameters	Values
Bulk volume, V_b, m^3	31.5×10^9
Porosity, ϕ	0.05
Recharge index, α, kg/bar.s	10
Initial mass fraction of CO_2, f_0	0.021
Total compressibility, c_t, bar^{-1}	1.7×10^{-4}
Production rate, w_p, kg/s	2000
Reinjection rate, w_{inj}, kg/s	1500
Reinjection mass fraction, f_{inj}	0
Water density, ρ_w, kg/m^3	876.19
Initial pressure, p_i, bar	150
Reinjection temperature of water, T_{inj}, ^oC	110

2.3.1 Comparison of κ values for the analytical and numerical solution

Figure 2.3 represents the results of the comparison between the analytical model which is given as Equation 2.13 and the numerical solution with respect to the analytical equation for various κ values such as 10^7, 2.4×10^8, 10^9. As a result, an excellent match is obtained between the models.

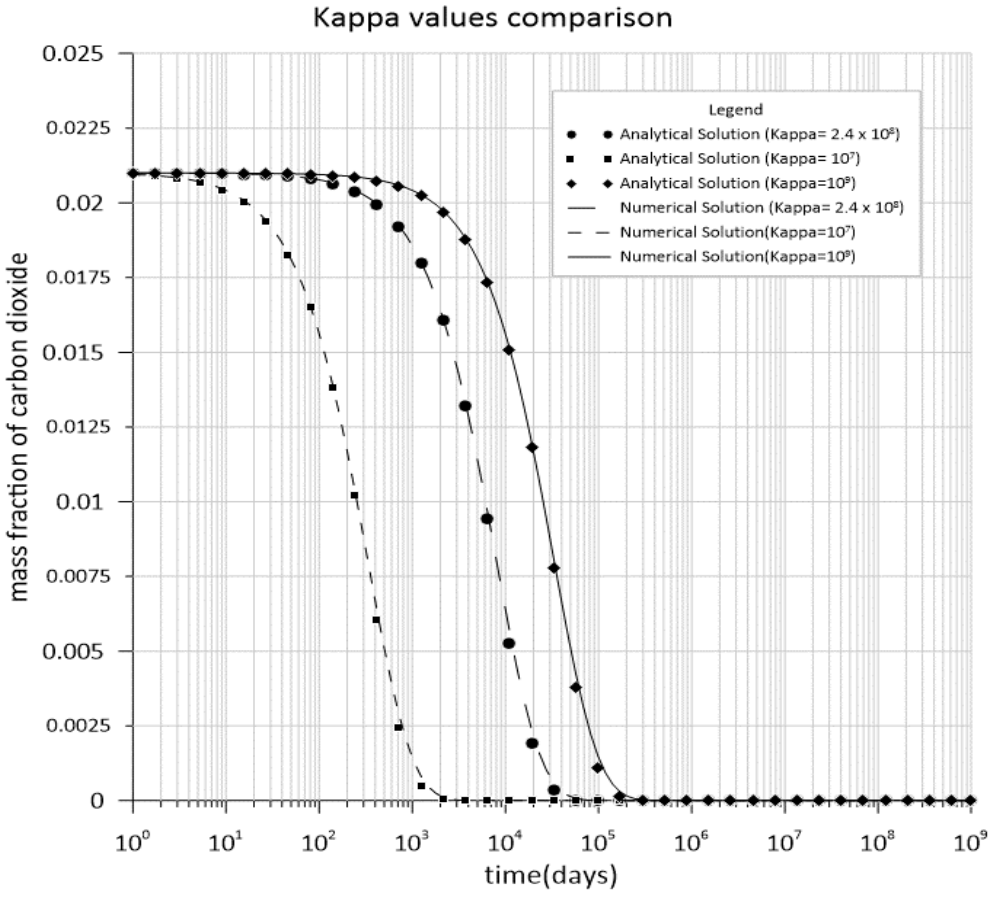

Figure 2.3 : κ values comparison.

2.3.2 Comparison of f_{re} values for the analytical and numerical solution

Figure 2.4 represents the analytical solution which is given as Equation 2.13 and the numerical solution with respect to the analytical equation for various f_{re} values such as 0, 0.0105 and 0.021. As a result, an excellent match is obtained between the models.

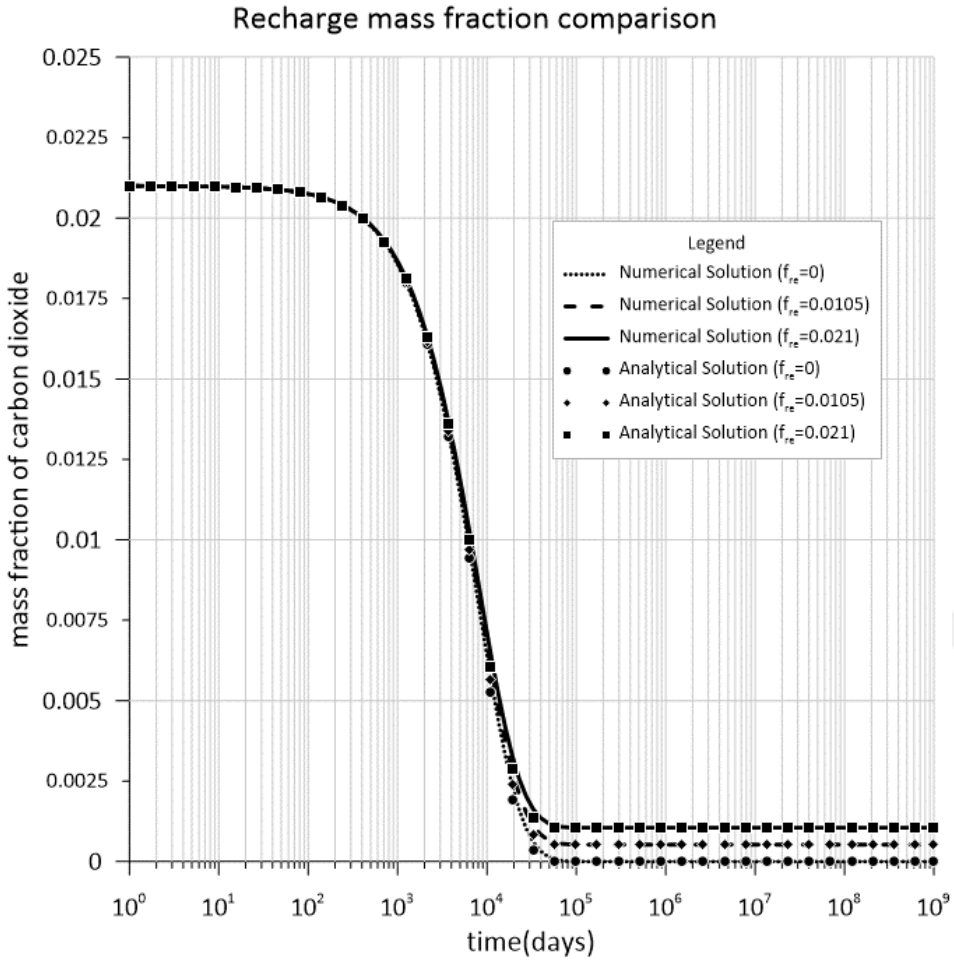

Figure 2.4 : f_{re} values comparison.

3. APPLICATIONS OF THE MODEL

In this chapter, various example applications of the model are provided. Synthetic applications regarding the production/reinjection strategy are given. In this section, we consider a case where the geothermal system is composed of two different regions, Region 1 and Region 2. Region 1 represents the part of the reservoir that is closer to the recharge source and Region 2 represents the part of the reservoir that is further away from the recharge source. The following scenarios are considered evaluating the production/reinjection strategies: For case 1, f_{re} = 0, also the production and reinjection operations are only for Region 2 while there is no production nor injection in Region 1 which is also shown in Figure 3.1. For case 2, f_{re} = 0, and, the production takes place in Region 2 whereas reinjection takes place in Region 1, which is shown in Figure 3.2. For case 3, f_{re} = 0.5%, and the production and reinjection operations are only for Region 2 while there is no production nor injection in Region 1 which is shown in Figure 3.3. For case 4, f_{re} = 0.5%; and, the production takes place in Region 2 whereas reinjection takes place in Region 1, which is shown in Figure 3.4. For case 5 f_{re} = 0, the production and reinjection operations are only for Region 1 while there is no production nor injection in Region 2 which is also shown as Figure 3.5. For case 6, f_{re} = 0, the production takes place in Region 1 whereas reinjection takes place in Region 2, which is shown in Figure 3.6. For case 7, f_{re} = 0.5 %, the production and reinjection operations are only for Region 1 while there is no production nor injection in Region 2 which is also shown in Figure 3.7. For case 8, f_{re} = 0.5 %, and the production takes place in Region 1 whereas reinjection takes place in Region 2, which is also shown as Figure 3.8.

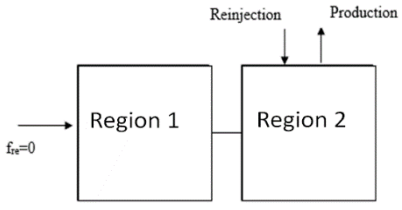

Figure 3.1 : Illustration of case 1.

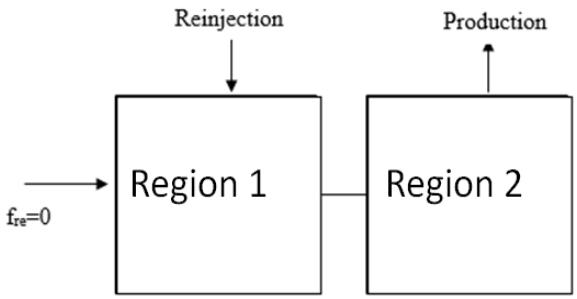

Figure 3.2 : Illustration of case 2.

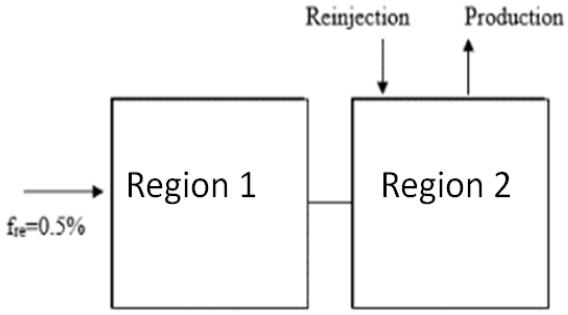

Figure 3.3 : Illustration of case 3.

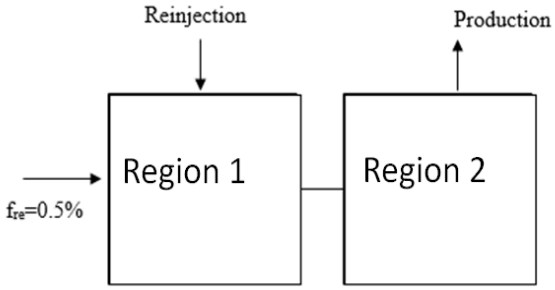

Figure 3.4 : Illustration of case 4.

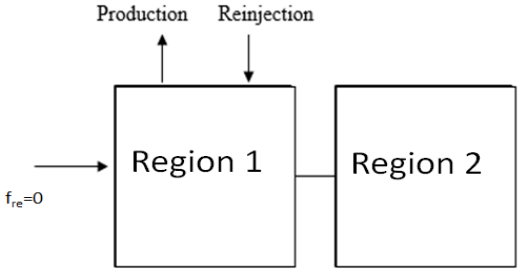

Figure 3.5 : Illustration of case 5.

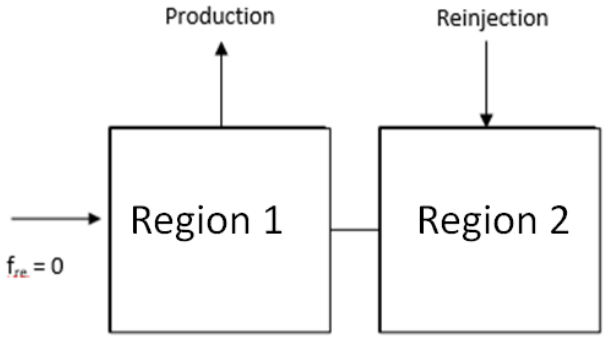

Figure 3.6 : Illustration of case 6.

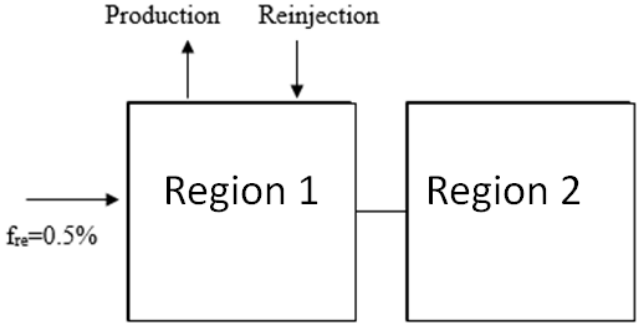

Figure 3.7 : Illustration of case 7.

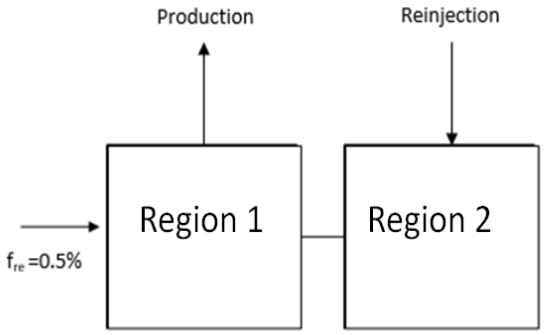

Figure 3.8 : Illustration of case 8.

Eight different production/reinjection scenarios which are illustrated above are discussed in detail in the following sections. The parameters that are used in these scenarios are given in Table 3.1.

Table 3.1 : Parameters used for different production/reinjection scenarios.

Parameters	Region 1	Region 2
Bulk volume, V_b, m^3	63×10^9	31.5×10^9
Porosity, ϕ	0.05	0.05
Rock Density,kg/m^3	2600	2600
Rock compressibility, bar^{-1}	94×10^{-6}	94×10^{-6}
Rock specific heat capacity, J/kg/ ^oC	1000	1000
Initial pressure, p_i, bar	150	150
Initial temperature, T_i, ^oC	200	200
Initial CO_2 mass fraction	0.021	0.021
Recharge index, kg/bar.s	40	-
Reinjection temperature, T_{inj}	110	110

For different production/reinjection scenarios, every case is investigated under the following assumptions:

- Diffusion of CO_2 because of concentration difference is ignored between the tanks.
- The recharge constant between the recharge source and Region 1 is taken equal to the recharge constant between Region 1 and Region 2.
- Initial pressures are the same for all of the regions.
- Porosities, rock densities, rock compressibilities, initial CO_2 mass fractions are the same in all of the regions.
- In all cases the production rate is taken as 2000 kg/s and the reinjection rate is taken as 1500 kg/s.

3.1 Production and Reinjection in Region 2 with f_{re}=0

The first case is where the mainly the production and reinjection operations takes place in Region 2. f_{re} is zero in this case. The model results are given in Figure 3.9. As it is clear from Figure 3.9 a decline in the CO_2 content is clearly observed. The decline is due to the fact that the reinjected CO_2 content is zero and also that the recharge CO_2 content is zero. At late times the CO_2 content stabilizes at a value of zero. This is again expected since, both reinjection and recharge CO_2 contents are zero. In other words, after stabilization there is no more CO_2 left in the reservoir. It is also observed that the decline of CO_2 content in Region 2 starts earlier. This is also expected because reinjection starts at the same time as production. In Region 1 however, the recharge water does not immediately start entering Region 1 because of the transient effects.

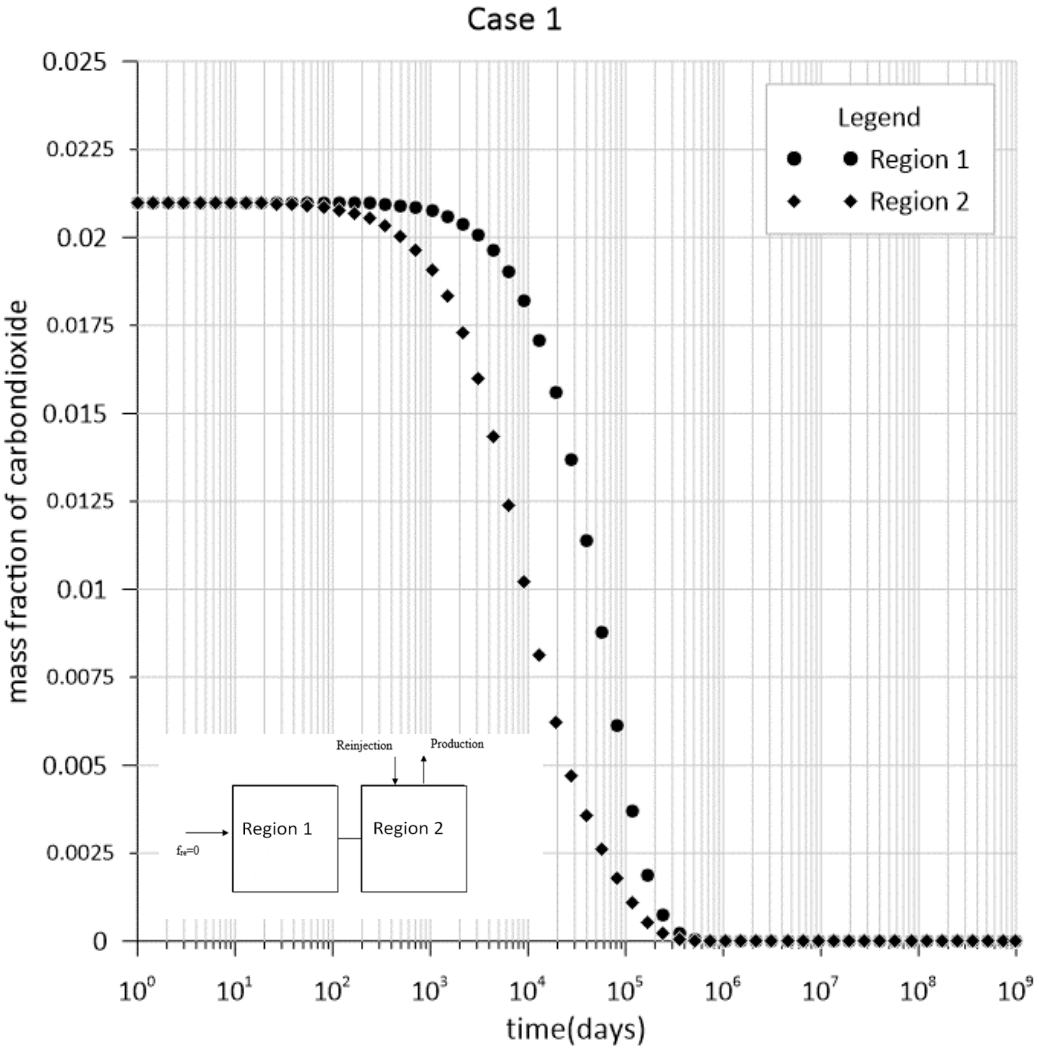

Figure 3.9 : Production and reinjection in Region 2 with f_{re}=0.

3.2 Production in Region 2 and Reinjection in Region 1 with f_{re}=0

The second scenario consists of both production and injection operations however separately in two tanks. The behavior of the mass fraction of two tanks can be seen in Figure 3.10. In this case, both CO_2 contents reaches zero again since both f_{re}=0 and f_{inj}=0. However, in Region 1, CO_2 content starts decreasing earlier. This is because reinjection in this case is into Region 1. Hence it starts declining earlier. For this case the only source of water with lesser CO_2 is Region 1. In other words Region 2 receives influx only from Region 1. Hence it takes a longer time for the CO_2 levels in Region 2 to decline. Another interesting observation is such that the stabilization of CO_2 levels seem to be occurring earlier when compared with the results of Figure 3.9. This is mainly due to the fact that reinjection is performed into Region 1 which causes less transient effect.

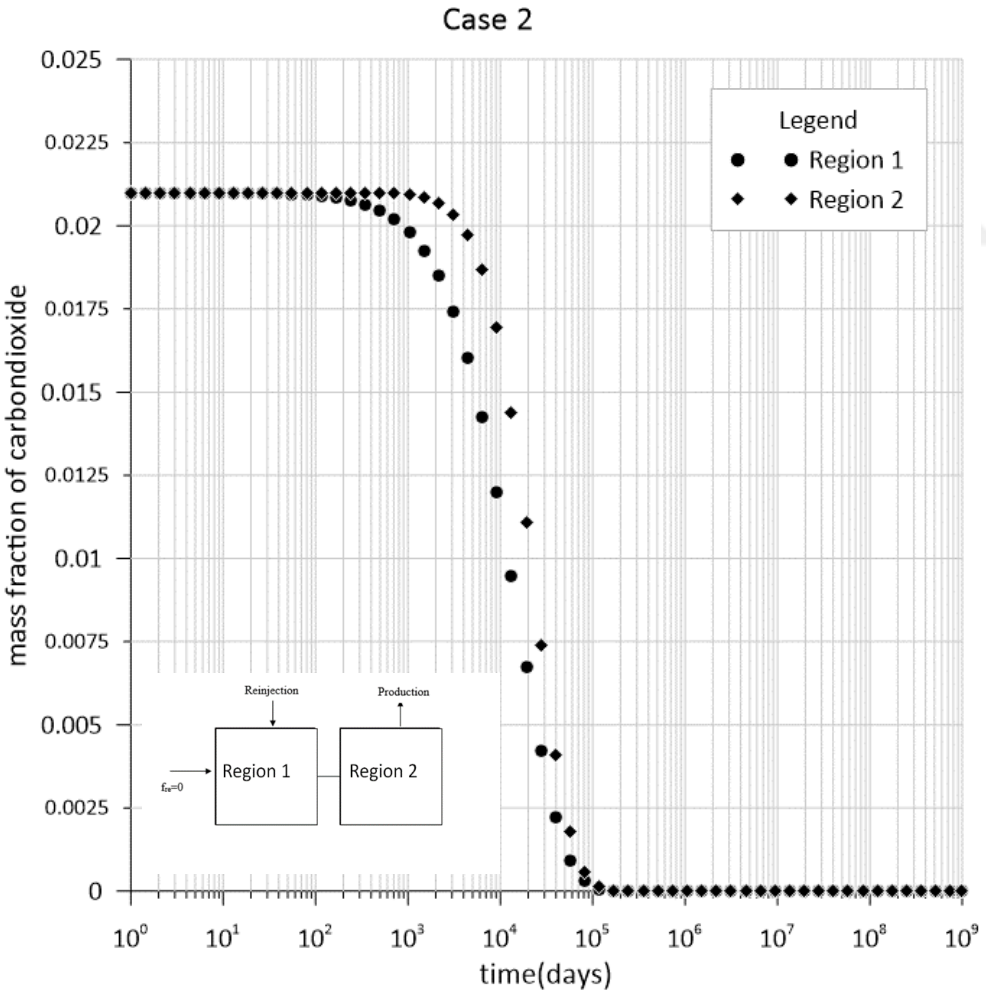

Figure 3.10 : Production in Region 2 and reinjection in Region 1 with f_{re}=0.

3.3 Production and Reinjection in Region 2 with f_{re}= 0.5%

Figure 3.11 illustrates the results for this case. The CO_2 content of both of the regions reaches different values in late times. Region 1 reaches 0.5% while the other one reaches 0.125%. The stabilized content of Region 1 is because of the fact that the only influx into Region 1 is from the recharge source which has a CO_2 content of 0.5%. Hence this CO_2 content mainly dictates the stabilized behaviour. The stabilized CO_2 content behaviour of Region 2 can best be explained by using Equation 2.14. At first it is important to note that at stabilized conditions the mass rate coming out of Region 2 will be equal to the mass rate going into Region 2. This implies that while the production and reinjection rates are 2000 kg/s and 1500 kg/s respectively, the total recharge rate into Region 2 will be their difference of 500 kg/s. The recharge CO_2 content in this case will be the stabilized content of Region 1 which is 0.5% or 0.005 by fraction. Applying Equation 2.14 yields a stabilized CO_2 content at 0.125% for Region 2. The reasoning for the early decline of the CO_2 content of Region 2 has been explanied previously in Case 1.

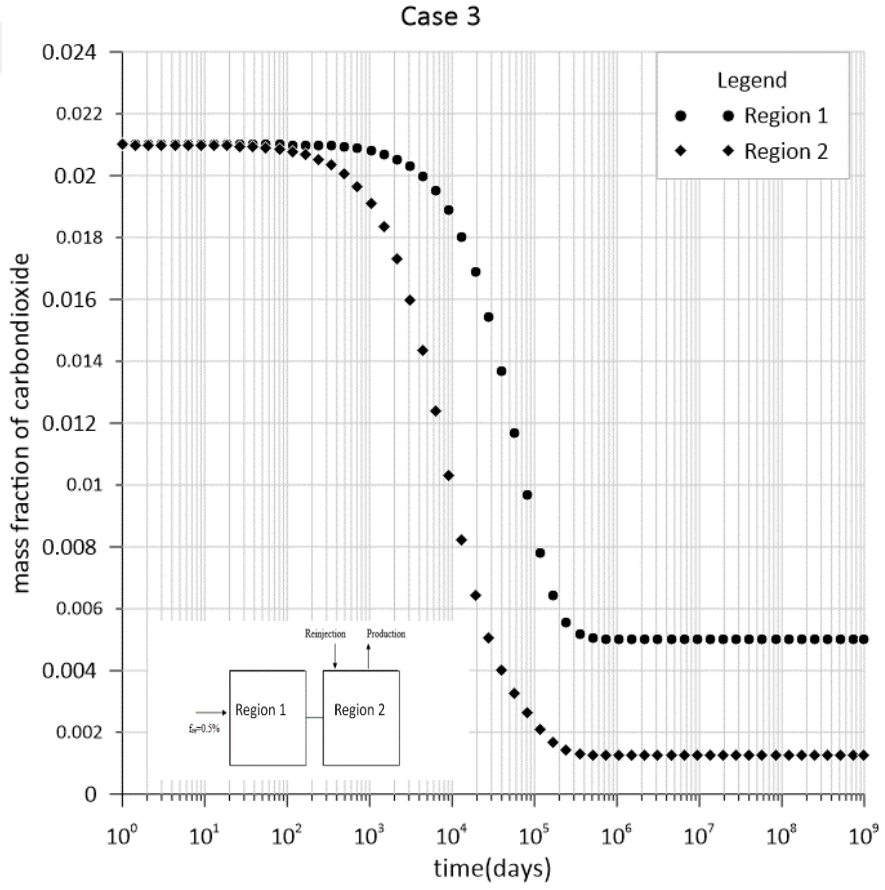

Figure 3.11 : Production and reinjection in Region 2 with f_{re}= 0.5%.

3.4 Production in Region 2 and Reinjection in Region 1 with f_{re}=0.5%

Figure 3.12 illustrates the case where production is in Region 2 and reinjection is in Region 1 with f_{re}=0.5%. The fact that Region 1 CO_2 content starts declining earlier has been explained previously in Case 2. As it is clear from Figure 3.12 both regions reach a stabilized CO_2 content of 0.0125. This behavior can again be explained using Equation 2.14. Lets first consider the stabilized CO_2 content of Region 1. At stabilized conditions the total mass rate out of Region 1 will be into Region 2 with a mass rate of 2000 kg/s. The mass rate going into Region 1 will be from both the recharge and the reinjection. Since at stabilized conditions, the mass going out must equal the mass going in, and that the reinjection rate is 1500 kg/s, then the recharge rate must equal 500 kg/s. With these figures if we use Equation 2.14, then the stabilized CO_2 content for Region 1 is 0.125%. When we consider Region 2 at stabilized conditions the recharge from Region 1 must be equal to the production rate of 2000 kg/s. Since the stabilized CO_2 content of Region 1 is 0.125% as computed previously, then the recharge into Region 2 will be at 0.125%. Hence Region 2 also stabilizes at a values of 0.125%.

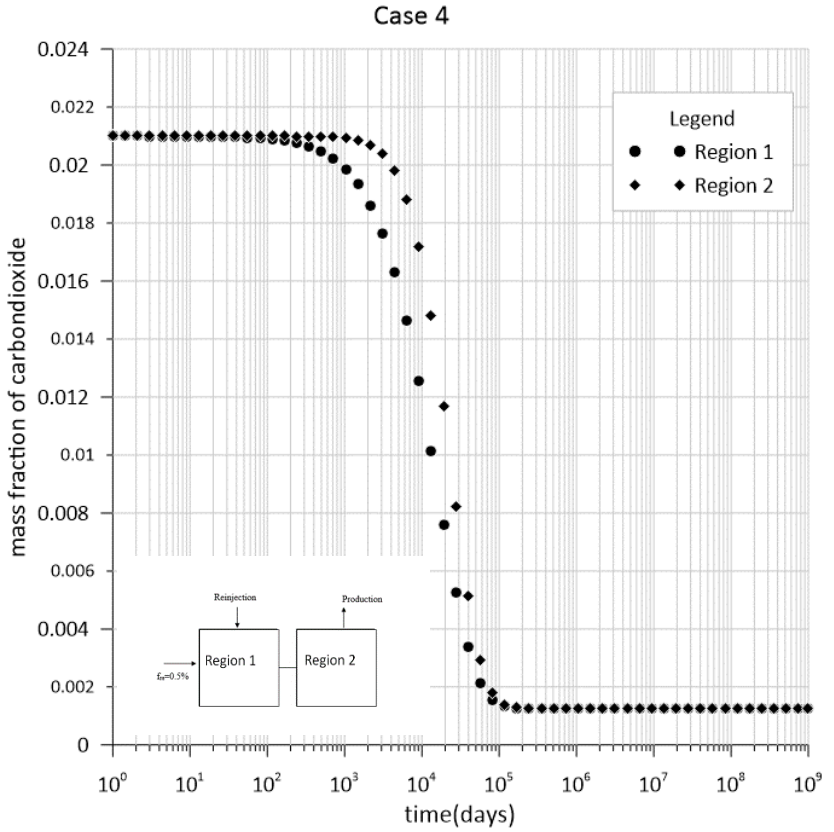

Figure 3.12 : Production in Region 2 and reinjection in Region 1 with f_{re}=0.5%.

3.5 Production and Reinjection in Region 1 with f_{re}=0

The results for this case is illustrated in Figure 3.13. As it is clear, the CO_2 content in Region 2 does not change with time and stays at the initial value. This is expected since no production/reinjection activity takes place in Region 2. As expected the CO_2 content of Region 1 declines to a stabilized values of zero since both the recharge CO_2 content and the reinjection content is zero.

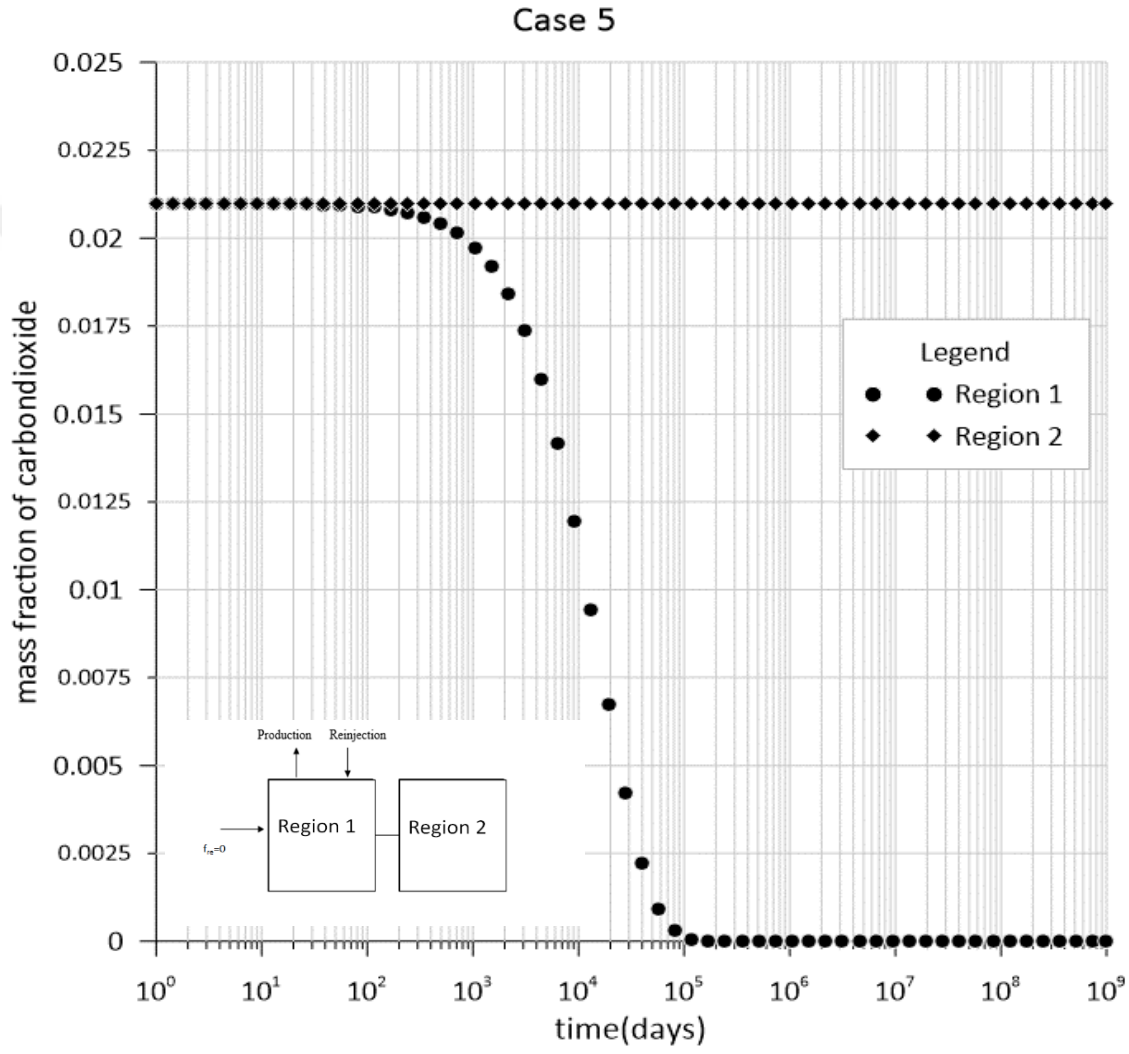

Figure 3.13 : Production and reinjection in Region 1.

3.6 Production in Region 1 and Reinjection in Region 2 with f_{re}=0

This case is illustrated in Figure 3.14 As it is seen the behavior of CO_2 content in both regions can be seen. The CO_2 content of CO_2 declines earlier in Region 2 since reinjection takes place in Region 2. Both Region 1 and Region 2 decline down to a stabilized value of zero since both recharge and reinjection CO_2 contents are zero.

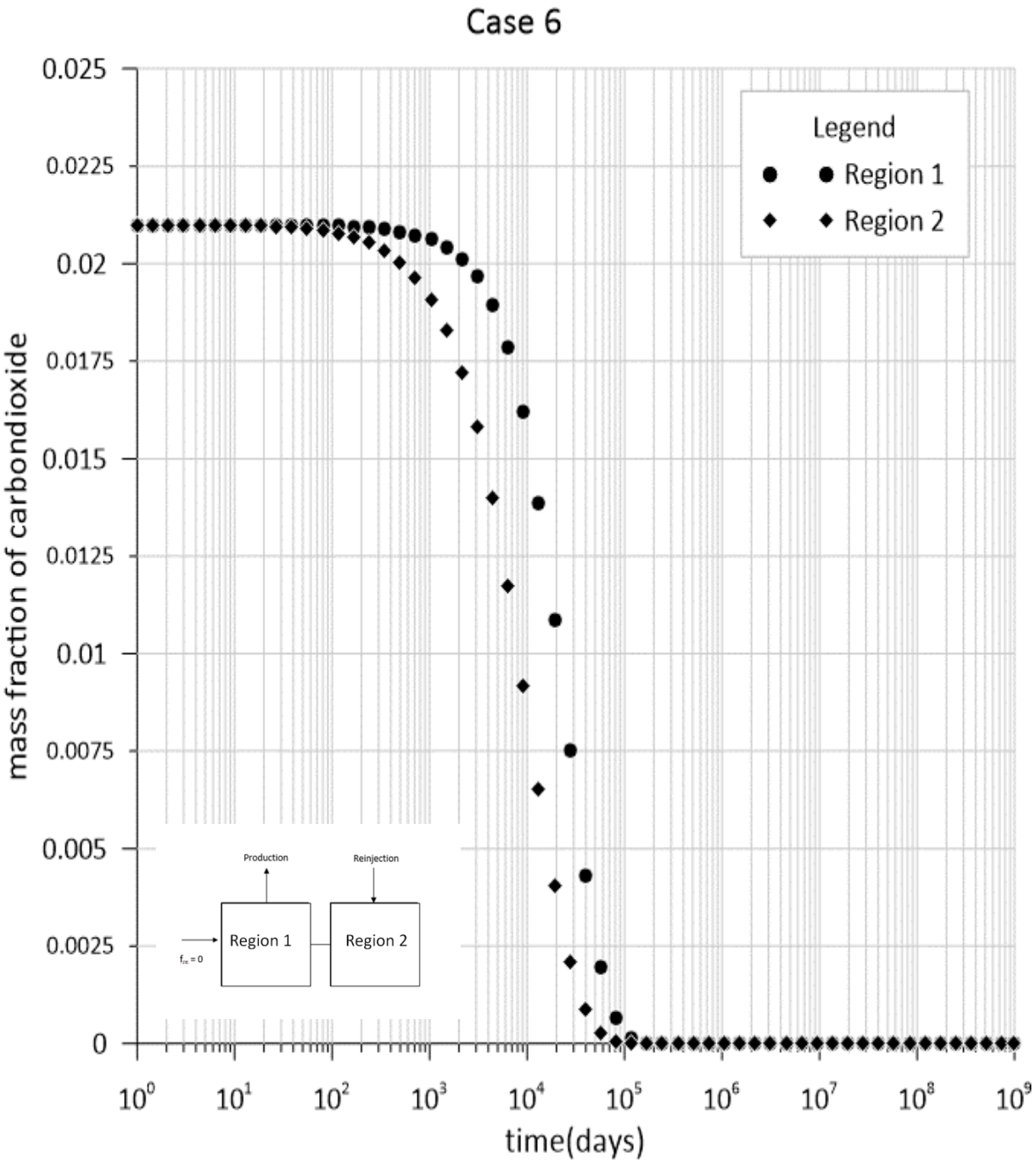

Figure 3.14 : Production in Region 1 and reinjection in Region 2.

3.7 Production and Reinjection in Region 1 with f_{re}= 0.5%

This case is illustrated in Figure 3.15, in this case, both production and reinjection are made at Region 1 with recharge contribution of f_{re}=0.5%. As it is clear Region 2 CO_2 content does not change since no production/reinjection is conducted in Region 2. As demonstrated earlier, Region 1 CO_2 content declines down to 0.125%. This result can also be verified with the application of Equation 2.14.

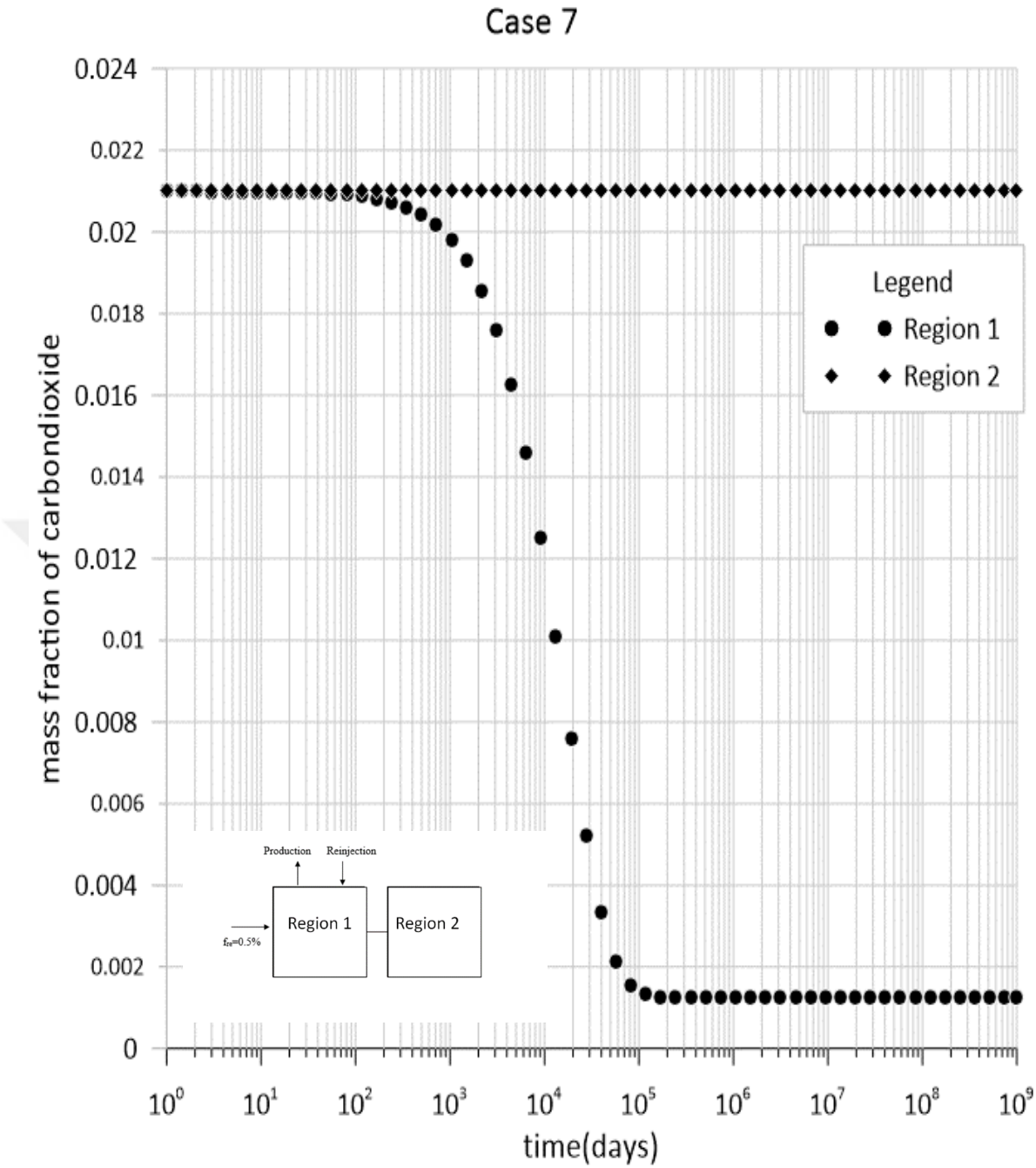

Figure 3.15 : Production and reinjection in Region 1.

3.8 Production in Region 1 and Reinjection in Region 2 *with* f_{re}= 0.5%

This case is illustrated in Figure 3.16. As it is seen from Figure 3.16, in Region 1, reinjection occurs while in Region 2 production occurs. As it is expected the mass fraction of CO_2 content due to production will fastly decrease in Region 2, and in Region 1. The amount of CO_2 content will be 0.125%. Justification for this value has been provided in the previous cases.

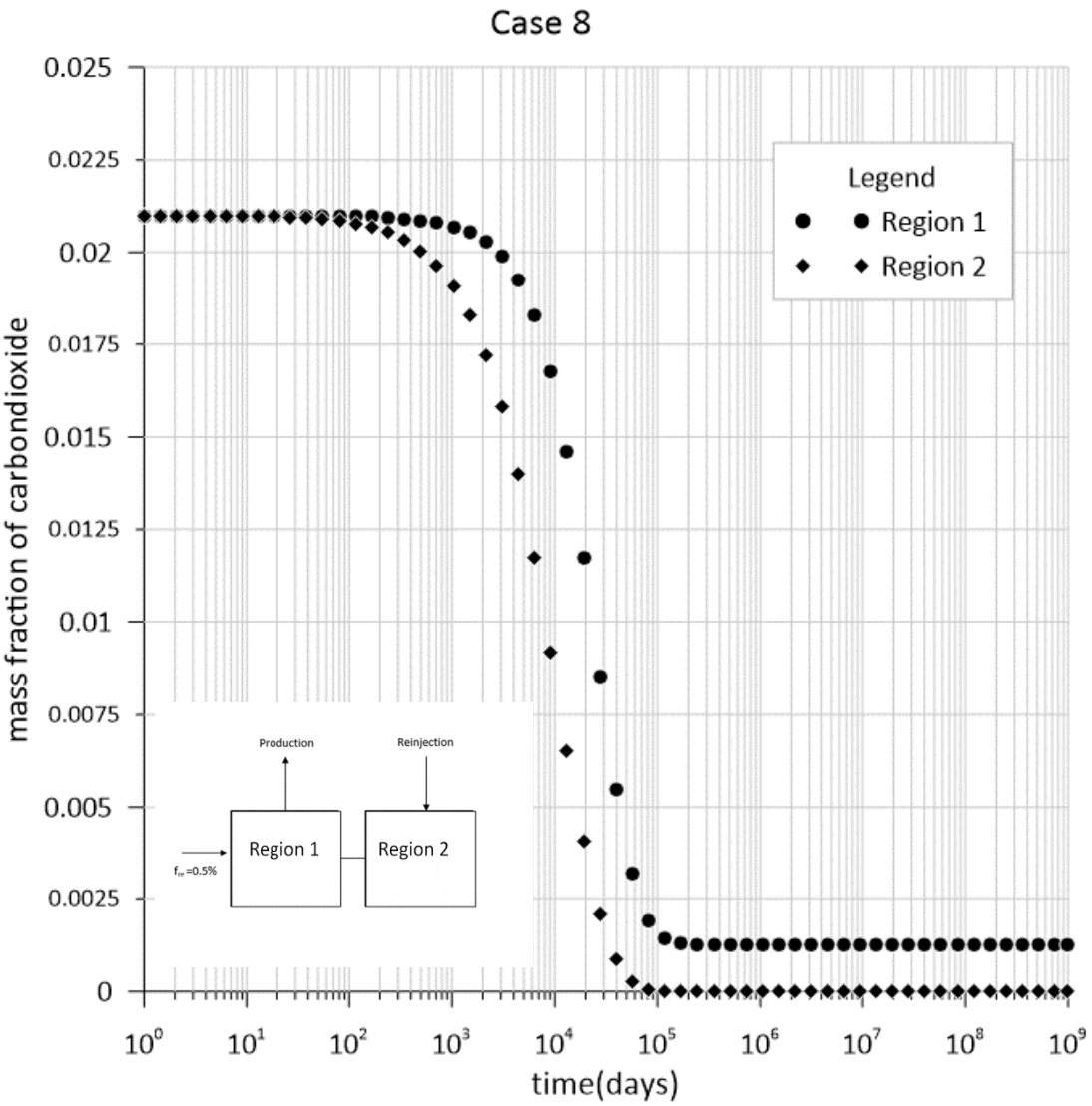

Figure 3.16 : Production in Region 1 and reinjection in Region 2.

4. CONCLUSIONS

In this study, a new model is developed for tracking the CO_2 content using lumped parameter models with multiple tanks. The basis of the model is such that mass balance on water, mass balance on CO_2 and an overall energy balance equation is solved simultaneously on all tanks. By solving the three conservation equations, pressure, temperature, and carbon dioxide behavior can be modeled for each tank under a given production/reinjection scenario. In this thesis, only the CO_2 content behavior is considered. This study specifically focuses on utilizing the model for various production/reinjection strategies given on a synthetic example. Eight different scenarios are considered in the synthetic example. In this synthetic example the geothermal reservoir is considered to be composed of two parts, a region that is farther away from the recharge source, and a region closer to the recharge source. Various scenarios are then considered where, in each scenario the locations of the production and reinjection operations are varied. The following conclusions have been obtained from this study:

- In all cases, the CO_2 content behavior reaches steady state at very long times. The time to reach steady state depends greatly on the κ value just as in the case of pressure stabilization. In the examples considered, the volumes of the tanks are taken to be comparable with that of actual sizes of reservoirs. If the tanks represent a smaller volume, such as the volume of a region where few wells exist, then it should be expected that stabilization times be reached at much earlier times.
- The steady state value of the CO_2 content depends on reinjection rate, production rate, the recharge CO_2 content and the reinjection CO_2 content.
- Since the reinjected CO_2 mass fraction is taken as zero for the case presented here, the region where reinjection is performed usually shows a factor decline of CO_2 content.

- If the recharge CO_2 content is higher, this leads to higher stabilized CO_2 content values in the reservoir.
- The model developed in this study does not consider the diffusion of CO_2 between the tanks. It should be noted that in the examples provided in this study, stabilized conditions are reached with continuing production/reinjection rates. In some cases, depending on the recharge CO_2 content, Region 1 and Region 2 reached different stabilized CO_2 contents. Based on the model, if production/reinjection was to stop, the model would not show any change, however in reality the CO_2 contents would change. However the diffusion of CO_2 is a slow process when compared with the change of CO_2 due to production/reinjection. Hence it is believed that not having the diffusion of CO_2 in the model will not affect the results.

REFERENCES

Acharya, H. (1983). Influence of plate tectonics on the locations of geothermal fields. *pure and applied geophysics,* Vol.*121,* Issue 5-6 , 853-867.

Aksoy, M. (2012). *Developments, Applications and Policies of Renewable Energy in Turkey,* Vol. *5*.

Alkan, H. and Satman, A. (1990). A new lumped parameter model for geothermal reservoirs in the presence of carbon dioxide. *Geothermics, 19,* 469-479.

Arps, J.J. (1945). Analysis of Decline Curves. *Trans. AIME*, vol. *160*, pp. 228-247.

Atkinson, P. G., Celati, R., Corsi, R. and Kucuk, F. (1980). Behavior of the Bagnore steam/CO_2 geothermal reservoir, Italy. *Society of Petroleum Engineers Journal, 20,* 228-238.

Axelsson, G. (1985). *Hydrology and thermomechanics of liquid-dominated hydrothermal systems in Iceland.* (PhD. Thesis). Oregon State University, Corvallis, Oregon.

Axelsson, G. (1989). Simulation of pressure response data from geothermal reservoir by lumped parameter models. *Proceedings of the 14th Workshop on Geothermal Reservoir Engineering*, 257-263, Stanford University, California.

Axelsson, G. and Dong, Z. (1998). The Tanggu geothermal reservoir (Tianjin, China). *Geothermics, 27,* Issue *3* , pp. 271-294.

Axelsson, G. and Gunnlaugsson, E. (2000). Long-term monitoring of high-and low-enthalpy fields under exploitation. *International Geothermal Association, WGC2000 Short Courses*, Kokonoe, Kyushu District, Japan, 28-30 May.

Bodvarsson, G.S., Pruess, K. and Lippmaan, M.J. (1986). Modeling of geothermal systems, *Journal of Petroleum Technology*, 1007-1021.

Breeze, P. (2014). Chapter 12 - Geothermal Power, *Power Generation Technologies (Second Edition)*, pp. 243-257.

Brigham, W. and Ramey Jr, H. (1981). Material and energy balance in geothermal reservoirs. *Reservoir Engineering Assessment of Geothermal Systems, Petroleum Engineering Department, Stanford University*.

Budd, C. F. Jr. (1972). Producing geothermal steam at the geysers field. *SPE Paper 4178 presented at Bekersfield*, California, Htg. Hov. 8-10.

Castanier, L.M. and Brigham, W.E. (1983). Use of lumped parameter modeling for geothermal engineering. *Proceedings of SPE California Regional Meeting*, Ventura, SPE 11730, 593-601, CA, USA, March 23-25.

Castanier, L. M., Sanyal, S. K., and Brigham, W. E. (1980). A practical analytical model for geothermal reservoir simulation. *Proceedings of the 50th Annual California Regional Meeting of SPE*. SPE 8887, 1-6, Los Angeles, CA, USA April 9-11.

Chierici, A. (1964). Planning of a geothermoelectric power plant: technical and economic principles. *Proc. U.N. Conf. New Sources Energy, Sol. Energy, Wind Power, Geotherm. Energy*, 1961 Vol. *4*, Pap. 9162, pp. 299-313.

Donaldson, I. G. , Grant, M. A. and Bixley, P. F. (1983). Nonstatic reservoirs: The natural state of the geothermal reservoir. *Journal of Petroleum Technology, 35*(1), 189-194.

Ghosh, T. K. and Prelas, M. A. (2011). Geothermal Energy. In *Energy Resources and Systems* ,pp. 217-266.

Grant, M. A. (1977). Broadlands - a gas dominated geothermal field. *Geothermics, 6*, no.p. 9-29.

Gringarten, A.C. and Sauty, J.P. (1975). A theoretical study of heat extraction from aquifers with uniform regional flow. *Journal of Geophysical Research, 80*, No. 35, 4956-4962, December 10.

Gudmundsson, J. and Olsen, G. (1987). Water-influx modeling of the Svartsengi geothermal field, Iceland. *SPE Reservoir Engineering*, pp. 77-84.

Haizlip, J. , M. Stover, M. , Garg, S. , Tut Haklidir, F. and Prina, N. (2016). Origin and Impacts of High Concentrations of Carbon Dioxide in Geothermal Fluids of Western Turkey. *Proceedings, 41st Workshop on Geothermal Reservoir Engineering*, Stanford University, Stanford, California.

Hoşgör, F. B. , Türeyen, Ö. İ. , Satman, A. and Çınar, M. (2015). Karbondioksitin Jeotermal Rezervuarların üretim performansı üzerindeki etkisi. *Proceedings, Ulusal Tesisat Mühendisleri Kongresi*, İzmir, Türkiye.

Hoşgör, F. B. , Tureyen, Ö. İ. and Satman, A. (2016). Keeping inventory of carbon dioxide in liquid dominated geothermal reservoirs. *Geothermics, 64*, 55-60.

Kaya, E., Onur, M. and Satman, A. (2005) Effects of CO_2 on reservoir and production performance of geothermal systems, *TPDD, 11*, 27-36.

Kaya, T. (2018). Türkiye'nin Enerji Görünümü. *TMMOB Makina Mühendisleri Odası, MMO/691*.

Melikoğlu, M. (2017). Geothermal energy in Turkey and around the World: A review of the literature and an analysis based on Turkey's Vision 2023 energy targets. *Renewable and Sustainable Energy Reviews, 76*, 485-492.

Michaelides, E. E. (2012). Geothermal Energy. In Alternative Energy Sources, Vol. 9, pp. 257–285.

Muffler, L.J.P. (1976). Tectonic and hydrological control of the nature and distribution of geothermal resources. *In: Proc. Second U.N. Symp. on*

the Development and Use of Geothermal Resources, California, U.S.A., 20-29 May 1975, 1: 499-- 508.

Olasolo, P. , Juárez, M. C. , Morales, M. P. , D´Amico, S. and Liarte, I. A. (2016). Enhanced geothermal systems (EGS): A review. *Renewable and Sustainable Energy Reviews, 56*, 133-144.

Olsen, G., (1984). Depletion Modeling of Liquid Dominated Geothermal Reservoir. Technical Report, *SGP-TR-80, Stanford Geothermal Program*, Stanford University, Palo Alto, California.

Onur, M., Sarak, H., Türeyen, Ö.İ., Çınar, M. and Satman, A. (2008). A new non-isothermal lumped parameter model for low temperature, liquid dominated geothermal reservoirs and its applications. *Proceedings 33rd Workshop on Geothermal Reservoir Engineering*, Stanford University, USA.

Richter, A. (2018). *Geothermal Energy in Europe and The Rest of The World.* Powerpoint presentation at the Geotermikonference, Christiansborg, Copenhagen, Denmark.

Sanyal, S. K. (2010). Future of geothermal energy. P*aper presented at the Proceedings of 35th Workshop on Geothermal Reservoir Engineering, Stanford University*, Stanford, California.

Sanyal, S.K., Sengul, M. and Mediav, H. T. (1976). A Semi-analytical approach to geothermal reservoir performance prediction. *2nd Workshop on Geothermal Reservoir Engineering Stanford University*, Palo Alto, California, December, 1-3.

Sarak, H., Onur, M., and Satman, A. (2005). Lumped-parameter models for low temperature geothermal reservoirs and their application. *Geothermics, 34*, 728-755.

Satman, A . (2018). Personal communication.

Satman, A. , Onur, M. , Serpen, U. and Aksoy, N. (2007). A Study on production and reservoir performance of Ömer-Gecek/Afyon geothermal field. *Proceedings, 32nd Workshop on Geothermal Reservoir Engineering, Stanford University*, Stanford, California.

Satman, A., Sarak, H., Onur, M. and Korkmaz, E.D. (2005). Modeling of production/reinjection behavior of the Kizildere geothermal field by a 2-Layer Geothermal Reservoir Lumped Parameter Model. *Proceedings, World Geothermal Congress*, Antalya, Turkey.

Satman, A. , Tureyen, O. , Korkmaz Basel, E. , Güney, A. , Senturk, E. and Kindap, A. (2017). Effect of Carbon Dioxide Content on the Well and Reservoir Performances in the Kizildere Geothermal Field. *Proceedings, 42nd Workshop on Geothermal Reservoir Engineering, Stanford University*, Stanford, California.

Schilthuis, R. J. (1936). Active oil and energy. *Trans. AIME, 118*, 33-52.

Serpen, Ü., Aksoy, N. and Öngür, T. (2010). 2010 Present status of geothermal energy in Turkey. *35th Workshop on Geothermal Reservoir Engineering Stanford University*, Stanford, California, February 1-3.

Şimşek, N. (1998). Enerji sorununun çözümünde jeotermal enerji alternatifi. *Ekoloji Çevre Dergisi, 8*, 15-20.

Stockton, A.D., Thomas, R.P. and Chapman, R.H. (1984). A reservoir assessment of the Geysers geothermal field. *Journal of Petroleum Technology*, *36*, 12, pp.2.137 - 2.159.

Tureyen, Ö. İ. and Akyapi, E. (2011). a generalized non-isothermal tank model for liquid dominated geothermal reservoirs. *Geothermics*, *40*, 50-57.

Tureyen, Ö.İ., Onur, M. and Sarak, H. (2009). A Generalized non-isothermal lumped parameter model for liquid dominated geothermal reservoirs. *Proceedings 34th Workshop on Geothermal Reservoir Engineering*, Stanford University, USA.

Url-1 < *https://www.e-education.psu.edu/marcellus/node/870*>, date retrieved 14.11.2018.

Url-2 < *http://www.bgs.ac.uk/research/energy/geothermal/home.html*>, date retrieved 14.11.2018.

Url-3 < *https://www.flickr.com/photos/105441355@N07/10918465575*>, date retrieved 14.11.2018.

Url-4 < *https://www.slideshare.net/NainHoney/geothermal-power-plant-and-its-types*>, date retrieved 14.11.2018.

Url-5 < *https://www.slideshare.net/NainHoney/geothermal-power-plant-and-its-types* >, date retrieved 14.11.2018.

Url-6 < *https://www.slideshare.net/NainHoney/geothermal-power-plant-and-its-types* >, date retrieved 14.11.2018

U.S Department of Energy. (2016). Enhanced Geothermal System (EGS) Fact Sheet. [PDF file]. Retrieved from https://www1.eere.energy.gov/geothermal/pdfs/egs_basics.pdf

Whiting, R. L. and Ramey, H. J. (1969). Application of material and energy balances to geothermal steam production. *Journal of Petroleum Technology*, *21*, 893-900.

Zaim, A. and Çavşi, H. (2018). Türkiye'deki Jeotermal Enerji Santrallerinin Durumu. *Engineer, 59*, 45-58.

CURRICULUM VITAE

Name Surname: Alper Süleyman Can

Place and Date of Birth: Istanbul, 1992

E-Mail: canal@itu.edu.tr

EDUCATION:

B.Sc.: 2016, Istanbul Technical University, Faculty of Mines, Geological Engineering (2010-2016).

OTHER PUBLICATIONS, INTERNSHIPS AND PATENTS :

- Anadolu Yer Bilimleri , 08.2012 - 09.2012
- Central Anatolian Tectonics project in collaboration with North Arizona University, 06.2015 – 07.2015.